

DISCONTINUITY FORMULAS FOR MULTIPARTICLE AMPLITUDES

Henry P. Stapp

Lawrence Berkeley Laboratory
University of California
Berkeley, California 94720

0. INTRODUCTION

I. PROPERTIES OF LANDAU SURFACES

1. Landau Diagrams D
2. Landau Equations Associated with D
3. Space-time Representations of D
4. Internal and External Variables
5. Landau Surfaces $L(D)$
6. Representations $D(p)$
7. Simple Points of $L(D)$
8. Basic Surfaces $L_0(D)$
9. Positive- α Diagrams and Surfaces
10. The Restricted Mass Shell \mathcal{M}^r
11. The Space $\mathcal{M}^4(p)$
12. The Sets \mathcal{M}_0 and \mathcal{M}'
13. Theorem 1
14. Theorem 2
15. Theorem 3
16. The $4n$ -Vector $u(D(p))$
17. The Functions $\phi(p; K(\bar{p}))$
18. The Physical Region $\mathcal{D}(D)$
19. Pham's Theorem
20. Theorem 4
21. Theorem 5
22. Analytic Submanifolds and Local Coordinate.

NOTICE -
This report was prepared as an account of work sponsored by the United States Government. Neither the United States Government nor the Lawrence Berkeley Research and Development Administration, nor any of their employees, nor any of their contractors, subcontractors, or their employees, makes any warranty, express or implied, or assumes any liability or responsibility for its accuracy, completeness or usefulness. It is the property of the United States Government and is loaned to the recipient. Its use, reproduction, disclosure, or transfer without the written consent of the United States Government is prohibited.

HENRY P. STAPP

II. BUBBLE DIAGRAM FUNCTIONS

1. Box Diagrams
2. The Cluster Decomposition
3. Bubble Diagrams \mathcal{B}
4. Bubble Diagram Functions F^B and Γ^B
5. Products of δ -functions
6. Condition for $J \neq 0$
7. Singularities Required by Unitarity

III. THE STRUCTURE THEOREM

1. The Normal Analytic Structure
2. Landau Diagrams That Fit into Bubble Diagrams
3. The Structure Theorem
4. The Physical Region of \mathcal{B}
5. $u = 0$ Points

IV. THE DISCONTINUITY OF f^+ AROUND $L_0(D^+)$

V. DERIVATION OF THE FORMULA FOR THE DISCONTINUITY OF f^+ AROUND $L_0(D^+)$

1. General Method
2. Pole-Factorization Theorem Below 4-Particle Threshold
3. Triangle Diagram Singularity
4. The Indented Box
5. Leading Normal Threshold Formula

VI. FORMAL METHOD

1. The Minus-Bubble Expansion of S
2. Formal Framework
3. Existence of $T(D^+)$ and $R(D^+)$
4. Uniqueness of $T(D^+)$ and $R(D^+)$
5. The Indented Box Revisited
6. Flowlines and Schnitts
7. Strongly Equivalent Schnitts

DISCONTINUITY FORMULAS

8. Nonleading Normal Threshold
9. Truncated Scattering Functions
10. The General Formula

VII. BASIC DISCONTINUITIES FOR 6-PARTICLE PROCESSES

1. The Sixteen Channels g
2. Signs of Lines $V_r \rightarrow V_s$
3. Theorem 14
4. Skeleton Diagrams
5. Theorem 15
6. Continuation of Good M^G 's Around Nonexceptional $L(D)$

IX. ANALYTICITY IN THE COMPLEX MASS SHELL

1. Maximal Analyticity
2. Hermitian Analyticity
3. Crossing
4. Triangle Diagram Cuts
5. Higher Cuts

DISCONTINUITY FORMULAS FOR MULTIPARTICLE AMPLITUDES*

Henry P. Stapp

Lawrence Berkeley Laboratory
University of California
Berkeley, California 94720

O. INTRODUCTION

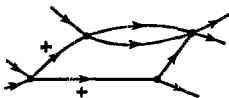
The aim of these lectures is to show how discontinuity formulas for multiparticle scattering amplitudes are derived from unitarity and analyticity. The assumed analyticity property is the normal analytic structure, which was shown in the previous lecture series to be equivalent to the space-time macrocausality condition. The discontinuity formulas to be derived are the basis of the multiparticle fixed- t dispersion relations, upon which the subsequent lecture series on Regge theory is based.

I. PROPERTIES OF LANDAU SURFACES

This section contains a brief review of the properties of Landau surfaces that are needed in the work that follows.

1. Landau Diagrams D

Example



A Landau diagram is a diagram formed from lines L_i and vertices V_r . Each line is directed from left to right. The topological structure of D is defined by the incidence matrix ϵ_{ir} :

$$\begin{aligned}\epsilon_{ir} &= -1 && \text{if } L_i \text{ originates on } V_r \\ \epsilon_{ir} &= +1 && \text{if } L_i \text{ terminates on } V_r \\ \epsilon_{ir} &= 0 && \text{otherwise}.\end{aligned}\quad (1.1)$$

Each line L_i is associated with a momentum-energy vector p_i , with a particle-type label t_i , and with a mass m_i characteristic of particles of type t_i . These masses m_i are assumed to be positive: $m_i > 0$. Each internal line L_i of D either carries a sign ϵ_i , plus or minus, or carries no sign.

2. Landau Equations Associated with D

For each Landau diagram D there is an associated set of Landau equations. These are

- (1) The mass-shell constraints: for each line L_i of D

$$p_i^2 = m_i^2, \quad p_i^0 > 0. \quad (2.1.1)$$

(2) The momentum-energy conservation-law constraints: for each vertex v_r of D

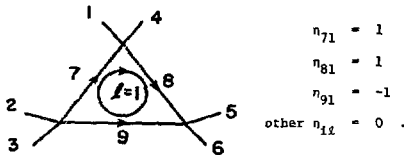
$$\sum_i p_i \epsilon_{ir} = 0. \quad (2.1.2)$$

(3) The Landau loop equations: for each directed closed loop ℓ that can be drawn on the internal lines of D

$$\sum_i a_i p_i n_{i\ell} = 0. \quad (2.1.3)$$

Each a_i is a scalar, and $n_{i\ell}$ is the number of times loop ℓ passes along line l_i moving in the direction of l_i minus the number of times it passes along l_i moving against the direction of l_i .

Example



$$(4) \text{ The nontriviality condition: for some internal line } l_i \quad a_i \neq 0. \quad (2.1.4)$$

$$(5) \text{ The sign conditions: for every signed line } l_i \quad a_i a_i > 0. \quad (2.1.5)$$

All variables are real unless otherwise stated.

3. Space-time Representations of D

For each solution $\{p_i, a_i\}$ of the Landau equations associated with D there is a space-time representation of D . This representation is a space-time diagram that has the topological structure of D . The vertex v_r of the representation lies at the space-time position w_r , and the vector from the origin of line l_i to its terminus, namely

$$\Delta_i \equiv \sum_r \epsilon_{ir} w_r, \quad (3.1)$$

satisfies

$$\Delta_i = a_i p_i. \quad (3.2)$$

The Landau loop equations entail the existence of a set of space-time vectors w_r such that (3.1) and (3.2) hold. Conversely, these two equations entail the

Landau loop equations.

The space-time representation can be interpreted as a classical multiple-scattering diagram for point particles. The conditions (3.1) and (3.2) are the classical condition $p_i = m_i v_i$, where v_i is the four-vector velocity of particle i : $v_i = dx_i/d\tau$. The sign condition $\sigma_i a_i > 0$ specifies that particle i move forward or backward in time according to whether σ_i is plus or minus.

4. Internal and External Variables

$$\begin{aligned} E_D &= \{i: L_i \text{ is an external line of } D\} \\ I_D &= \{i: L_i \text{ is an internal line of } D\} \\ p &= \{p_i: i \in E_D\} \\ \hat{p} &= \{p_i: i \in I_D\} \\ a &= \{a_i: i \in I_D\} \end{aligned}$$

5. Landau Surfaces $L(D)$

$L(D)$ is the set of points (p, \hat{p}, a) such that the Landau equations associated with D are satisfied. The Landau surface $L(D)$ is the projection of $\hat{L}(D)$ onto p space:

$$L(D) = \{p: (p, \hat{p}, a) \text{ satisfies the Landau equations associated with } D \text{ for some } (\hat{p}, a)\}. \quad (5.1)$$

6. Representations $D(p)$

A representation of D whose external lines are associated with the set $(p_1, \dots, p_n) \in p$ of momentum-energy vectors is denoted by $D(p)$. Each $D(p)$ generates the point p on $L(D)$, in the sense that represents a solution (p, \hat{p}, a) of the Landau equations associated with the Landau diagram D . The Landau surface $L(D)$ is the set of p such that some $D(p)$ exists:

$$L(D) = \{p: \text{some } D(p) \text{ exists}\}. \quad (6.1)$$

Given any $D(p)$ there is a five-fold continuum of others obtained from it by dilations (positive scale changes $\sigma_i \rightarrow \lambda \sigma_i, \lambda > 0$) and overall space-time translations. These transformations are called the trivial transformations.

7. Simple points of $L(D)$

A simple point p of $L(D)$ is a point p such that $D(p)$ is unique, modulo the trivial transformations: only one representation of D , modulo these trivial transformations, generates the point p .

8. Basic Surfaces $L_0(D)$

$$\begin{aligned} L_0(D) &= \{p: p \text{ is simple point of } L(D)\} \\ &= \{p: p \text{ is generated by only one representation of } D, \text{ modulo the trivial transformations}\}. \end{aligned}$$

9. Positive- α Diagrams and Surfaces

A Landau diagram D is called a positive- α diagram if and only if each internal

line of D carries a positive sign $\sigma_i = +$. A superscript plus on D^+ indicates that this diagram is a positive- α diagram. Landau surfaces $L(D^+)$ corresponding to positive- α diagrams are called positive- α Landau surfaces.

10. The Restricted Mass Shell \mathcal{M}^r

Let $p \in (p_1, \dots, p_n)$ be the set of momentum-energy vectors associated with the full set of initial and final particles of some scattering process. The corresponding restricted mass shell is

$$\mathcal{M}^r = \{p: p_1^2 = m_1^2, p_1^0 > 0, \sum_{i=1}^n \epsilon_i p_i = 0, \text{ and at least one pair of } p_i \text{ are nonparallel}\}. \quad (10.1)$$

The sign ϵ_i is plus for final L_i and minus for initial L_i .

The complex restricted mass shell \mathcal{M}_c^r is defined in the same way except that p is complex and the positivity condition $p_1^0 > 0$ is dropped.

11. The Space $\mathcal{M}^L(p)$

The set of vectors normal to the mass shell \mathcal{M}^r at point p is called $\mathcal{M}^L(p)$:

$$\mathcal{M}^L(p) = \{u: u \cdot \delta(ep) = 0 \text{ for all } \delta(ep) \text{ in the tangent space to } \mathcal{M}^r \text{ at } p\} \quad (11.1)$$

$$= \{u = (u_1, \dots, u_n): u_1 = \lambda_1 p_1 + d, d \text{ is any four-vector, } \lambda_1 \text{ is any scalar}\}. \quad (11.2)$$

For any u in $\mathcal{M}^L(p)$ one has

$$u \cdot \delta(ep) = \sum_{i=1}^n u_i \cdot \delta(\epsilon_i p_i) = \sum_{i=1}^n (\lambda_i p_i + d) \cdot \epsilon_i \delta p_i = 0, \quad (11.3)$$

since the δp_i are subject to the constraints $\delta(p_i^2 - m_i^2) = 0$, and

$\delta(\sum \epsilon_i p_i) = 0$. For any two four-vectors a and b

$$a \cdot b = a^0 b^0 - \vec{a} \cdot \vec{b}. \quad (11.4)$$

12. The Sets \mathcal{M}_0 and \mathcal{M}'

\mathcal{M}_0 is the subset of \mathcal{M}^r such that two or more initial p_i are parallel or two or more final p_i are parallel. The set \mathcal{M}' is \mathcal{M}^r minus \mathcal{M}_0 :

$$\mathcal{M}' = \mathcal{M}^r - \mathcal{M}_0. \quad (12.1)$$

13. Theorem 1 Each nonempty set $L_0(D^+) \cap \mathcal{M}'$ is a codimension-one analytic submanifold of \mathcal{M}' .

Meaning: For any \bar{p} in $L_0(D^+) \cap \mathcal{M}'$ there is real function $\phi(p)$ such that (i) $\phi(p)$ is analytic at \bar{p} , (ii) the gradient $\nabla \phi(p)$ at \bar{p} lies outside $\mathcal{M}^L(\bar{p})$, and (iii) $L_0(D^+) \cap \mathcal{M}'$ coincides with $\{\phi(p) = 0\} \cap \mathcal{M}'$ in

some sufficiently small neighborhood of \bar{p} .

14. Theorem 2

$$L^+ = \bigcup_{D^+} L(D^+) = \bigcup_{D^+} L_0(D^+) .$$

15. Theorem 3

Only a finite number of D^+ give surfaces $L_D(D^+)$ that intersect any bounded portion of \mathcal{M}^r .

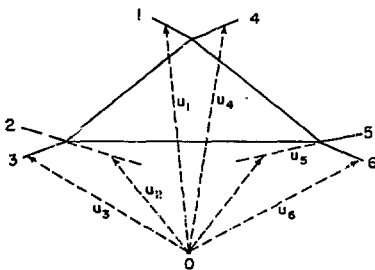
These three theorems, taken together, say that $L^+ \cap \mathcal{M}'$ consists of a locally finite union of codimension-one analytic submanifolds. Thus $L^+ \cap \mathcal{M}'$ is the union of a set of smooth surfaces: it has no cusps, acnodes or other irregularities.

References for the proofs of these and other theorems are given in a section at the end of the lectures.

16. The 4n-Vector $u(D(p))$

Let $D(p)$ be a space-time representation with N external lines. Then $u(D(p)) = u \equiv (u_1, \dots, u_n)$ is a set of n four-vectors u_i such that u_i is the vector from some arbitrary origin O to some arbitrary point on the space-time line that contains the trajectory of external particle i .

Example



Given any $D(p)$ there are others obtained from it by the trivial transformations. Also, the location of the end point of u_1 on the line containing L_1 can be changed. These changes alter the scale of u and add increments of the form

$$u_0(p) = (\lambda_1 p_1 + d, \dots, \lambda_n p_n + d) , \quad (15.1.1)$$

where the p_i are the momentum-energy vectors of the external lines of $D(p)$. The set of vectors $u_0(p)$ is just the set of vectors

$$u_0(p) \in \mathcal{M}^L(p) . \quad (15.1.2)$$

17. The Functions $\phi(p; D(\bar{p}))$

For any space-time representation $D(\bar{p})$ define

$$\begin{aligned} \phi(p; D(\bar{p})) &= (\epsilon p - \epsilon \bar{p}) \cdot w(D(\bar{p})) \\ &= \sum_{i \in E_D} (\epsilon_i p_i - \epsilon_i \bar{p}_i) \cdot w_{r(i)}(D(\bar{p})) \end{aligned} \quad (17.1)$$

where $v_{r(i)}$ is the vertex of D connected to external line i , and $w_{r(i)}(D(\bar{p}))$ is the location of v_r in the representation $D(\bar{p})$. The function $\phi(p; D(\bar{p}))$ is a linear function of p that vanishes at $p = \bar{p}$ and has at \bar{p} the gradient

$$\nabla \phi(\bar{p}; D(\bar{p})) = u(D(\bar{p})) + u_0(\bar{p}) , \quad (17.2)$$

where $u_0(p)$ lies in $\mathcal{M}^L(\bar{p})$.

18. The Physical Region $\mathcal{P}(D)$

$\mathcal{P}(D)$ is the set of points p such that for some (p, \bar{p}) the mass-shell and conservation-law conditions (2.1.1) and (2.1.2) in the Landau equations associated with D can be satisfied. The surface $L(D)$ clearly lies in $\mathcal{P}(D)$:

$$L(D) \subset \mathcal{P}(D) . \quad (18.1)$$

19. Pham's Theorem

For any representation $D^+(\bar{p})$ of D^+

$$\mathcal{P}(D^+) \subset \{p: \phi(p; D^+(\bar{p})) \geq 0\} . \quad (19.1)$$

Proof For brevity write $w_r(D^+(\bar{p})) = \bar{w}_r$, and identify also any other quantities pertaining to the representation $D^+(\bar{p})$ by a bar. Then for any p in $\mathcal{P}(D^+)$

$$\phi(p; D^+(\bar{p})) = \sum_{i \in E_D} (p_i - \bar{p}_i) \epsilon_i \bar{w}_{r(i)}$$

$$= \sum_{i \in E_D} \sum_r - (p_i - \bar{p}_i) \epsilon_{ir} \bar{w}_r$$

$$= \sum_{i \in E_D} \sum_r (p_i - \bar{p}_i) \epsilon_{ir} \bar{w}_r$$

(Equation continued next page)

(Equation continued)

$$\begin{aligned}
 &= \sum_{i \in I_D} (p_i - \bar{p}_i) \bar{a}_i \\
 &= \sum_{i \in I_D} (p_i - \bar{p}_i) \bar{a}_i \bar{p}_i \geq 0 . \quad (19.2)
 \end{aligned}$$

The final step in (19.2) follows from the fact that for any two positive-energy mass-shell vectors p_i and \bar{p}_i

$$p_i \cdot \bar{p}_i \geq \bar{p}_i \cdot \bar{p}_i = m_i^2 . \quad (19.3)$$

Remark 1 The last line of (19.2) expresses $\phi(p; D^+(\bar{p}))$ in terms of the internal variables associated with the solution of the Landau equation at \bar{p} . The p_i in this expression can be any set of internal p_i that satisfy the mass-shell and conservation law constraints. The fact that $\phi(p; D^+(\bar{p}))$ does not depend on the particular choice of these internal p_i is a consequence of the Landau loop equation.

20. Theorem 4 Consider any point \bar{p} on $L_0(D^+) \cap \mathcal{M}'$. Let $\phi(p)$ be as in Theorem 1. Then the sign of $\phi(p)$ can be chosen so that

$$\nabla \phi(p) \in u(D^+(\bar{p})) , \quad (20.1)$$

where \in means equal modulo positive scale changes and additions of vectors $u_0(p) \in \mathcal{M}^L(\bar{p})$.

Proof The set $L_0(D^+) \cap \mathcal{M}'$ lies in $\mathcal{P}(D^+) \cap \mathcal{M}'$. Thus $\{\phi(p) = 0\} \cap \mathcal{M}'$ lies in $\{\phi(p; D^+(\bar{p})) \geq 0\} \cap \mathcal{M}'$. The gradient $\nabla \phi(\bar{p})$ lies outside $\mathcal{M}^L(\bar{p})$, by virtue of Theorem 1, and the gradient $\nabla \phi(\bar{p}; D^+(\bar{p}))$ lies outside $\mathcal{M}^L(\bar{p})$ by virtue of the positive- α conditions, the stability conditions, and the condition that \bar{p} lie outside \mathcal{M}_0 . For these conditions entail that the (appropriately extended) external trajectories cannot pass through a common point, which they would if $\nabla \phi(p; D^+(\bar{p}))$, and hence $u(D^+(\bar{p}))$, lay in $\mathcal{M}^L(\bar{p})$. But if both these gradients lie outside $\mathcal{M}^L(\bar{p})$ then they must be the same, modulo scale changes, sign changes, and vectors of $\mathcal{M}^L(\bar{p})$, in order to accomodate the inclusion of $\{\phi(p) = 0\} \cap \mathcal{M}'$ in $\{\phi(p; D^+(\bar{p})) \geq 0\} \cap \mathcal{M}'$. This result entails (20.1).

Remark Two functions $\phi(p)$ that are analytic at \bar{p} , that have gradients lying outside $\mathcal{M}^L(\bar{p})$, and that give the same regions $\{\phi(p) \geq 0\} \cap \mathcal{M}'$ near \bar{p} are equivalent insofar as the defining properties of $\phi(p)$ are concerned. Thus if $\phi(p)$ is acceptable, and $\psi(p)$ is analytic at \bar{p} and vanishes on \mathcal{M}' then $\lambda \phi(p) + \psi(p)$ is also acceptable, provided λ is positive. The gradient $\nabla \phi(\bar{p})$ lies in $\mathcal{M}^L(\bar{p})$, hence $\nabla \phi(\bar{p}) \in \nabla(\lambda \phi(\bar{p}) + \psi(\bar{p}))$. Thus the significant part of $\nabla \phi(\bar{p})$ is defined only modulo positive scale changes and additions of vectors

$$u_0(\bar{p}) \in \mathcal{M}^L(\bar{p}).$$

The result $\nabla\phi(\bar{p}) = u(D^+(\bar{p}))$ is the origin of much of the importance of the space-time diagrams. It says that the normal to the Landau surface $L_0(D^+)/\mathcal{M}'$ at \bar{p} is essentially determined by the locations of the external space-time trajectories of any space-time representation $U(\bar{p})$ of D^+ that generates \bar{p} . This fact eliminates, in many situations, the need to actually calculate the Landau surface: the essential information can be extracted directly from the space-time representation.

2. Theorem 5 If two basic surfaces $L_0(D_1^+)$ and $L_0(D_2^+)$ coincide near $\bar{p} \in \mathcal{M}'$, then

$$u(D_1^+(\bar{p})) = u(D_2^+(\bar{p})). \quad (21.1)$$

(The equality of signs entailed by (21.1) rules out a clash of i.e. rules for coincident surfaces $L_0(D_1^+)$ and $L_0(D_2^+)$.)

22. Analytic Submanifolds and Local Coordinates

The restricted complex mass-shell \mathcal{M}_c^r is a $3n-4$ dimensional analytic submanifold of the space \mathbb{C}^{4n} of the n complex four-vectors p_i . This means that for each point \bar{p} of \mathcal{M}_c^r one can introduce a set of $4n$ functions $z_1(p), \dots, z_{4n}(p)$ that are analytic and functionally independent at \bar{p} (i.e., the $4n$ gradient vectors exist and are linearly independent at \bar{p}) such that the image under the mapping $z(p)$ of any sufficiently small complex mass-shell neighborhood of \bar{p} is an open set in the space \mathbb{C}^{3n-4} defined by $z_{3n-4+i} = 0$ for $i = 1, \dots, n+4$. The analyticity and functional independence of the $z_i(p)$ at \bar{p} entails that the inverse mapping $p(z)$ is uniquely defined and analytic near the image \bar{z} of \bar{p} . Thus sufficiently small neighborhoods of \bar{p} and \bar{z} are one-to-one analytic images of each other, with mass-shell neighborhoods mapping onto neighborhoods in \mathbb{C}^{3n-4} .

The functions $z_{3n-4+i}(p)$ for $i = 1, \dots, n+4$ can be taken to be the n functions $p_i^2 - m_i^2$, and the four functions $\sum \epsilon_i p_i^\mu = 0$, $\mu = 0, \dots, 3$. The gradients of these $n+4$ functions can easily be shown to be linearly independent for all points p in \mathcal{M}_c^r . This fact ensures that the remaining set of $3n-4$ functions $z_i(p)$ can be found. These latter coordinates (z_1, \dots, z_{3n-4}) are called local coordinates of the mass shell at \bar{p} .

The surface $L_0(D^+)/\mathcal{M}'$ is a codimension-one analytic submanifold of \mathcal{M}' . It coincides locally with the set $\{\phi(p) = 0\} \cap \mathcal{M}'$, where $\nabla\phi(\bar{p})$ lies outside $\mathcal{M}^L(\bar{p})$. This last condition ensures that the function $z_1(p)$ can be taken to be $\phi(p)$, since its gradient at \bar{p} is linearly independent of the $n+4$ gradients $\nabla z_{3n-4+i}(\bar{p})$. In this local coordinate system the singularity surface

$L_0(D) \cap \mathcal{M}'$ is just the surface $z_1 = 0$, restricted to the space \mathbb{C}^{3n-4} of local coordinates. The physical region $\mathcal{P}(D^+)$ near \bar{p} is mapped into the intersection of \mathbb{C}^{3n-4} with the ray

$$\operatorname{Re} z_1 \geq 0, \quad \operatorname{Im} z_1 = 0. \quad (22.1)$$

II. BUBBLE DIAGRAM FUNCTIONS

Topological considerations arising from the cluster decomposition of the S-matrix play a central role in the derivation of discontinuity formulas. Consequently it is helpful to represent certain important functions by diagrams, rather than by letters.

I. Box Diagrams The S-matrix is represented by a plus box, and its hermitian conjugate is represented by a minus box:

$$S(p_1, \dots, p_m; p_{m+1}, \dots, p_n) \equiv \begin{array}{c} 1 \\ \vdots \\ m \end{array} \text{---} \boxed{+} \text{---} \begin{array}{c} m+1 \\ \vdots \\ n \end{array} \quad (1.1.1)$$

$$S^\dagger(p_1, \dots, p_m; p_{m+1}, \dots, p_n) \equiv \begin{array}{c} 1 \\ \vdots \\ m \end{array} \text{---} \boxed{-} \text{---} \begin{array}{c} m+1 \\ \vdots \\ n \end{array} \quad (1.1.2)$$

The unit operator is represented by an I-box:

$$I(p_1, \dots, p_m; p_{m+1}, \dots, p_n) \equiv \begin{array}{c} 1 \\ \vdots \\ m \end{array} \text{---} \boxed{I} \text{---} \begin{array}{c} m+1 \\ \vdots \\ n \end{array} \quad (1.1.3)$$

The unitarity equation

$$\begin{aligned} \oint S(p_1, \dots, p_m; p'_1, \dots, p'_N) S^\dagger(p'_1, \dots, p'_N; p_{m+1}, \dots, p_n) \\ = I(p_1, \dots, p_m; p_{m+1}, \dots, p_n) \end{aligned}$$

is written

(1.1.4)

The shaded strip between the plus and minus boxes stands for a sum consisting of all possible numbers N of intermediate lines, and there is an implied summation over all distinct sets of variables associated with these lines:

$$\mathcal{F} = \sum_{i=1}^N \sum_{t_1} \int \prod_{i=1}^N \frac{d^4 p'_i}{(2\pi)^4} (2\pi) \delta^+(p'_i - m_i^2) \Theta . \quad (1.1.5)$$

Here Θ is a normal-ordering theta function that excludes from the region of integration all points $p' = (p'_1, \dots, p'_N)$ that differ only by the ordering of the variables p'_i from points already included in the region of integration.

Alternatively, Θ can be taken to be the inverse of the symmetry number of the diagram. This number is the number of symmetry operations that take the diagram into itself. In particular, for the term on the left-hand side of (1.1.4) having N intermediate lines the symmetry number is $N!$, provided the particle types t_i associated with the intermediate lines are not predetermined, and hence the sum includes for each internal line i a sum over all particle types t_i . The external lines of a diagram are considered to be distinguishable.

2. The Cluster Decomposition

Each box is written as a sum over all topologically different ways of connecting the fixed external lines to a set of bubbles. For example

$$\begin{aligned}
 \begin{array}{c} | \\ 1 \\ 2 \\ 3 \\ 4 \\ \hline + \\ 5 \\ 6 \\ 7 \\ 8 \end{array} &= \begin{array}{c} | \\ 1 \\ 2 \\ 3 \\ 4 \\ \hline + \\ 5 \\ 6 \\ 7 \\ 8 \end{array} + \sum_{(16)} \begin{array}{c} \text{two bubbles} \\ \text{with a line} \end{array} \\
 &+ \sum_{(72)} \begin{array}{c} \text{two bubbles} \\ \text{with a line} \end{array} + \sum_{(36)} \begin{array}{c} \text{two bubbles} \\ \text{with a line} \end{array} \\
 &+ \sum_{(4!)} \begin{array}{c} \text{two bubbles} \\ \text{with a line} \end{array}
 \end{aligned}$$

This is the cluster decomposition of S . The order (from top to bottom) in which the lines are connected to a bubble is not a topological distinction, nor is the (vertical) order in which the bubbles are placed on the paper. The number of diagrams in each partial sum in (2.1) is given below the summation sign. Within the bubbles occurring in the cluster decomposition of the plus (resp. minus) box is placed a plus (resp. minus) sign, except that no sign is placed inside the trivial bubbles, which are those with exactly one incoming line and exactly one outgoing line. The nontrivial bubbles with one or zero incoming lines or with one or zero outgoing lines are omitted, because of stability requirements.

The cluster decomposition of the I-box is similar, except that only trivial bubbles are allowed. Thus if the box on the left-hand side of (2.1) were an I-box then the right-hand side would be reduced to the final sum of $4!$ terms.

The plus and minus bubbles represent the connected parts of S and S^\dagger , respectively:

$$\begin{array}{c} \text{Diagram of a plus bubble with } m \text{ incoming lines and } m+1 \text{ outgoing lines} \\ \text{Diagram of a minus bubble with } m \text{ incoming lines and } m+1 \text{ outgoing lines} \end{array} = F^+(p) = S_c(p_1, \dots, p_m; p_{m+1}, \dots, p_n) \quad (2.2)$$

and

$$\begin{array}{c} \text{Diagram of a minus bubble with } m \text{ incoming lines and } m+1 \text{ outgoing lines} \\ \text{Diagram of a plus bubble with } m \text{ incoming lines and } m+1 \text{ outgoing lines} \end{array} = F^-(p) = S^\dagger(p_1, \dots, p_m; p_{m+1}, \dots, p_n) \quad (2.3)$$

Sometimes (see below) the minus bubble is defined to be minus the function defined above. Then in each term of the cluster decomposition of the minus box there is an extra factor $(-1)^{N^-}$, where N^- is the number of minus bubbles in that term, and (2.3) is replaced by

$$\begin{array}{c} \text{Diagram of a minus bubble with } m \text{ incoming lines and } m+1 \text{ outgoing lines} \\ \text{Diagram of a plus bubble with } m \text{ incoming lines and } m+1 \text{ outgoing lines} \end{array} = F^-(p) = -S_c^\dagger(p_1, \dots, p_m; p_{m+1}, \dots, p_n) \quad (2.3')$$

The trivial bubble represents the same function in the decomposition of the plus, minus, and I boxes:

$$i \longrightarrow j = (2\pi)^3 2p_i^0 \delta^3(\vec{p}_i - \vec{p}_j) \delta_{t_i t_j} \quad (2.4)$$

Each term in the cluster decomposition represents the product of the functions represented by the individual bubbles in that term. Thus each of the $4!$ terms

in the final sum in (2.1) is a product of four factors of the type (2.4).

Particles with spin can be included by regarding particles with different z components of spin as different types of particles. Fermions can be included by introducing a minus sign for each crossing of fermion lines in a diagram.

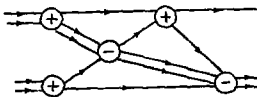
The connected parts F^+ and F^- each contain a conservation-law delta function. The functions f^+ and f^- are defined by

$$F^\pm(p) = (2\pi)^4 \delta^4(\sum e_i p_i) f^\pm(p) \quad (2.5)$$

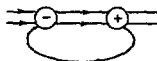
These functions $f^+(p)$ and $f^-(p)$ are called the scattering function and the hermitian conjugate scattering function, respectively.

3. Bubble Diagrams B

Example



Generally a bubble diagram B is a diagram consisting of signed bubbles connected by directed lines. Each bubble has two or more lines entering on its left side and two or more lines leaving from its right side. Each line runs always from left to right. This last condition excludes, for example,



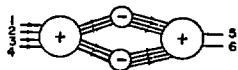
from the class of bubble diagrams.

4. Bubble Diagram Functions F^B and f^B

Each bubble diagram B represents a function F^B , which is the product of the functions F^+ or F^- corresponding to the bubbles of B , integrated over all distinct values of the variables corresponding to the internal lines of B .

This integration has the same form and normalization as (1.1.5), where $\#$ can now be taken to be the inverse of the symmetry number N_B . This number N_B is the number of symmetry operations that take B into itself.

Example If B is



then N_B is $3!3!4!4!2!$. The $2!$ comes from the symmetry under interchange of the two minus bubbles. The other four factors come from the symmetries under interchanges of the internal lines within each of the four sets of internal lines. In calculating the symmetry number of a diagram the external lines are considered distinguishable.

With this normalization the bubble diagram functions occurring in the equations we consider will always occur with coefficients plus or minus one.

F^B contains an overall conservation-law delta function, and f^B is defined by

$$F^B = (2\pi)^4 \delta^4(\sum_i p_i) f^B. \quad (4.1)$$

5. Products of δ -Functions

A bubble diagram function F^B will generally contain a product f of scattering functions f^+ and f^- times a product of mass-shell and conservation-law delta functions. A product of delta functions is generally defined by transforming to a set of integration variables that includes the arguments of the delta functions:

$$\begin{aligned} & \int f \prod_{i=1}^m \delta(g_i(x)) dx_1 \cdots dx_n \\ &= \int f \prod_{i=1}^m \delta(g_i(x)) dg_1 \cdots dg_n J^{-1} \\ &= \int f dg_{m+1} \cdots dg_n J^{-1}, \end{aligned} \quad (5.1)$$

where $J = |dg/dx|$ is the Jacobian of the transformation. This procedure is legitimate provided J is nonzero throughout the domain of integration.

6. Condition for $J \neq 0$

Near any point x in the domain of integration one can find a set of functions $g_{m+1}(x), \dots, g_n(x)$ such that $J \neq 0$ unless the m gradient vectors v_{g_1}, \dots, v_{g_m} are linearly dependent at x . To find the $J \neq 0$ conditions for a bubble diagram function F^B first eliminate the conservation-law delta

functions by expressing the p_i in terms of the loop momenta k_i ,

$$p_i = \sum n_{i\ell} k_\ell + p_i^{\text{ex}}, \quad (6.1)$$

where p_i^{ex} is a function of the external momenta. Then the arguments of the remaining delta functions are the functions

$$g_i(k, p_i^{\text{ex}}) = p_i^2(k, p_i^{\text{ex}}) - m_i^2. \quad (6.2)$$

The gradients $\nabla_k g_i$ of these functions are linearly dependent if and only if for some set of a_i , not all zero,

$$\sum_i a_i \nabla_k g_i = 0. \quad (6.3)$$

The insertion of (6.2) and (6.1) in (6.3) gives for each loop ℓ the equation

$$\sum_i a_i p_i n_{i\ell} = 0. \quad (6.4)$$

These equations (6.4) are just the Landau loop equations for the Landau diagram $D(B)$ constructed by shrinking each bubble of B to a point. Thus the product of the mass-shell and conservation-law delta functions occurring in F^B is well defined away from the Landau surface $L(D(B))$. The function F^B is expected to be singular at $L(D(B))$. It will also have other singularities arising from the singularities of the functions f^+ and f^- themselves. The structure theorem to be described in Section III specifies the possible locations of singularities of bubble diagram functions.

7. Singularities Required by Unitarity

Consider $3 \rightarrow 3$ unitarity:

$$\begin{array}{c}
 \text{Diagram with } + \text{ in circle} - \text{ in circle} = \text{Diagram with } + \text{ in circle } - \text{ in circle} \\
 - \quad \text{Diagram with } - \text{ in circle} \\
 + \sum_f \text{ Diagram with } + \text{ in circle } - \text{ in circle } f \\
 + \sum_i \text{ Diagram with } + \text{ in circle } - \text{ in circle } i \\
 + \sum_{i,f} \text{ Diagram with } + \text{ in circle } - \text{ in circle } i f
 \end{array} \quad (7.1)$$

(Convention (2.3') is used here.)

Can we assume that all scattering functions f^+ and f^- are everywhere analytic? No, this is not compatible with unitarity. For the bubble diagram functions on the right-hand side of (7.1) would then contain singularities that could not cancel among themselves (provided the relevant f^\pm 's are not identically zero, in which case other unitary equations could be considered). Thus unitarity requires some of the functions f^\pm to have singularities (since we know they are not all identically zero).

The normal analytic structures (NAS) described in Professor Iagolnitzer's lectures does not require scattering functions to have any singularities: it says only that the allowed singularities lie on L^\pm . Thus we have

- (i) Unitarity requires some singularities;
- (ii) NAS allows only certain singularities.

Questions

- (1) Is NAS consistent with unitarity?
- (2) If so, which of the singularities allowed by NAS are forced to be present by unitarity?
- (3) Can one derive the discontinuity formulas just from unitarity and NAS?
- (4) If so, what are these formulas?

The present work is addressed to these questions.

III. THE STRUCTURE THEOREM

The structure theorem describes certain analyticity properties of bubble diagram functions that follow from the normal analytic structure of scattering functions. This theorem plays a fundamental role in the derivation of discontinuity formulas.

1. The Normal Analytic Structure

- (a) $f^+(p)$ is analytic in $\mathfrak{M}^r - L^+$.
- (b) $f^+(p)$ at $\bar{p} \in \mathfrak{M}^r \cap L^+$ is the boundary value of an analytic function from any direction in the tangent space to \mathfrak{M}_c^r at \bar{p} that lies in the cone

$$C^+(\bar{p}) = \bigcap_{D^+(\bar{p})} \{ \bar{p} + iq: \operatorname{Im} \phi(\bar{p} + iq; D^+(\bar{p})) > 0 \} \quad (1.1)$$

The cone $C^+(\bar{p})$ is the intersection of the "upper-half planes" associated with all the positive- α diagrams $D^+(\bar{p})$ that generate \bar{p} . Properties (a) and (b) also hold if f^+ is replaced by f^- , provided the sign of ϕ in (1.1) is reversed.

The precise meaning of properties (a) and (b) is defined by introducing a set $z = (z_1, \dots, z_{3n-4})$ of local coordinates of \mathfrak{M}_c^r at \bar{p} . Property (a) says that if the mapping $z(p)$ is restricted to some sufficiently small neighborhood

of \bar{p} then $f^+(p(z))$ is analytic in the z -space image $z(\eta^r - L^+)$ of $\eta^r - L^+$. This property is independent of the particular choice of local coordinates $z_1(p), \dots, z_{3n-4}(p)$.

Property (b) is expressed in terms of the vectors

$$\begin{aligned} u(D^+(\bar{p})) &= \left. \nabla_p \phi(p; D^+(\bar{p})) \right|_{p=\bar{p}}, \\ &= \nabla \phi(\bar{p}; D^+(\bar{p})) \end{aligned} \quad (1.2)$$

or more precisely, their z -space images

$$\begin{aligned} u'(D^+(\bar{p})) &= \left. \nabla_z \delta(p(z); D^+(\bar{p})) \right|_{z=z(\bar{p})=\bar{z}} \\ &= \nabla \delta(\bar{p}(\bar{z}); D^+(\bar{p})) \end{aligned} \quad (1.3)$$

The components of u' are related to those of u by

$$u'_i = \sum_j u_j \left. \frac{\partial p_i}{\partial z_j} \right|_{z=z(\bar{p})=\bar{z}}. \quad (1.4)$$

The cone of vectors $u'(D^+(\bar{p}))$ has in $y = \text{Im } z$ space a dual cone

$$C^+(\bar{z}) = \bigcap_{D^+(\bar{p})} \{y: y \cdot u'(D^+(\bar{p})) > 0\}. \quad (1.5)$$

Let C be any nonempty open cone (with apex at $y = 0$) that is contained with its boundary in $C^+(\bar{z}) \cup \{y = 0\}$. Then property (b) asserts that there is a complex neighborhood η of \bar{z} and a function $f^+(z)$ that (1) is analytic in $\eta \cap \{\text{Im } z \in C\}$, and (2) coincides in the limit $\text{Im } z \rightarrow 0$ with the distribution $f^+(p(x))$ in $\eta \cap \{\text{Im } z = 0\}$, in the sense that for any test function $\chi(x)$ with support in $\eta \cap \{\text{Im } z = 0\}$

$$\int f^+(p(x)) \chi(x) dx = \lim_{y \rightarrow 0} \int f^+(x + iy) \chi(x) dx. \quad (1.6)$$

Moreover, any decomposition of the set of vectors $u'(D^+(\bar{p}))$ into closed convex cones \sum_i (with apex at the origin) induces a corresponding decomposition of f near \bar{p} into distributions f_i such that each $f_i(p(x))$ near $x = \bar{x}$ is the boundary value of a function $f_i(z)$ from almost all directions in the dual cone

$$C_i^+(\bar{z}) = \bigcap_{D^+(\bar{p}) \in \sum_i} \{y: y \cdot u'(D^+(\bar{p})) > 0\},$$

in the manner analogous to that described above.

Claim (b) depends on the function $\phi(p; D^+(p))$ only via the direction of the z -space image $u'(D^+(\bar{p}))$ of $u(D^+(\bar{p}))$. Any $u \in \mathcal{M}^+(\bar{p})$ has an image $u' = 0$, since the vectors $\partial p / \partial z_i$ occurring in (1.4) lie in the tangent space to \mathcal{M}^+ at \bar{p} .

The expression (1.1) for $C^+(\bar{p})$ can be simplified by using the following theorem:

Theorem 6 For any representation $D^+(\bar{p})$ the vector $u(D^+(\bar{p}))$ can be expressed as the finite sum

$$u(D^+(\bar{p})) = \sum_i \lambda_i u(D_i^+(\bar{p})) \quad , \quad (1.7)$$

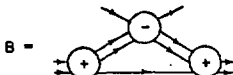
where the λ_i are nonnegative scalars and the D_i^+ are the diagrams that are contained in D^+ and satisfy $\bar{p} \in L_0(D_i^+)$. A diagram D_1^+ is contained in D_2^+ if and only if D_2^+ contracts to D_1^+ .

This result is closely connected to Theorem 2. To prove it one may first use the argumentation in Pham's theorem to conclude that all representations $D^+(\bar{p})$ of D^+ that generate \bar{p} must have the same set of internal momenta \hat{p} , and then, by considering the range of the α 's, identify the diagrams D_i^+ as the various contractions of D^+ at \bar{p} that cannot be further contracted.

This result allows, in Eq. (1.1), the sum over all $D^+(\bar{p})$ to be reduced to a sum over all $D^+(\bar{p})$ such that $\bar{p} \in L_0(D^+)$.

2. Landau Diagrams That Fit into Bubble Diagrams

Example



D fits into B .

Generally a Landau diagram D is said to fit into bubble diagram B if and only if D can be constructed by inserting into each bubble b of B either a connected Landau diagram D_b or a point vertex D_b . The initial and final lines of D_b must coincide with the incoming and outgoing lines of b , in the natural one-to-one fashion indicated in the example, and each internal line L_i of D_b must carry a sign ω_i that coincides with the sign of b . The external lines of the various D_b , which are all explicit lines of B , are left unsigned.

A superscript B on D means that this Landau diagram D fits into B .

3. The Structure Theorem

Theorem If the NAS holds then

(a) $f^B(p)$ is analytic in $\mathcal{M}^r - L^B$, where

$$L^B = \bigcup_{D^B} L(D^B), \quad (3.1)$$

and

(b) $f^B(p)$ at $\bar{p} \in \mathcal{M}_c^r \cap L^B$ is the boundary value of an analytic function from any direction in the tangent space to \mathcal{M}_c^r at \bar{p} that lies in the cone

$$C^B(\bar{p}) = \bigcap_{D^B(\bar{p})} \{ \bar{p} + iq: \text{Im } \phi(\bar{p} + iq; D^B(\bar{p})) > 0 \}. \quad (3.2)$$

This result for the bubble diagram function f^B is completely analogous to the NAS: the superscript $+$ is merely replaced throughout by the superscript B . Claim (b) is void if $C^B(p)$ is empty or fails to intersect the tangent space to \mathcal{M}_c^r at \bar{p} .

4. The Physical Region of B

The physical region of B , called $\mathcal{P}(B)$, is the region outside L^B due to the mass-shell and conservation-law constraints occurring in its definition. These constraints are the same as those associated with the bubble diagram $D(B)$ obtained by shrinking the bubbles of B to points. Hence

$$\mathcal{P}(B) = \mathcal{P}(D(B)) \quad (4.1)$$

and

$$F^B(p) = 0 \text{ for } p \text{ outside } \mathcal{P}(B). \quad (4.2)$$

The function $F^B(p)$ is generally nonzero inside $\mathcal{P}(B)$. Thus it cannot generally be the limit of a single analytic function in any real neighborhood of a point $\bar{p} \in L(D(B))$. Hence claim (b) of the structure theorem must be void for $\bar{p} \in L(D(B))$.

This is indeed the case. Since every bubble of $D^B = D(B)$ is contracted

to a point, no line of D^B carries a sign. Thus for any representation $D^B(\bar{p})$ another can be constructed by reversing the signs of all a_i . The signs of the vectors $u(\bar{p})$ and $w(\bar{p})$ are also reversed, hence so is the sign of $\phi(p; D^B(\bar{p}))$. Thus if \bar{p} lies on $L_0(D^B)$ the cone $C^B(\bar{p})$ is empty, and claim (b) is void.

5. $u = 0$ points

Suppose there is a $D^B(\bar{p})$ such that

$$u(D^B(\bar{p})) = 0$$

or equivalently such that

$$u'(D^B(\bar{p})) = 0. \quad (5.1)$$

Then $C^B(\bar{p})$ does not intersect the tangent space to \mathcal{M}_c^F at \bar{p} , and claim (b) is void.

A point \bar{p} such that (5.1) holds is called a $u = 0$ point. Such points sometimes cover open sets. However, in the many cases studied so far the function f^B is not actually singular on these open sets. Thus the structure theorem, in its present form is inadequate at $u = 0$ points: it permits singularities that are not actually present.

This inadequacy of the present version of the structure theorem is circumvented in the present work by introducing a perhaps needless assumption, as will be discussed later.

IV. THE DISCONTINUITY OF f^+ AROUND $L_0(D^+)$

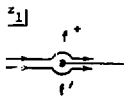
Let D^+ be a positive- α diagram, and let $\bar{p} \in \mathcal{M}'$ be a point that lies on $L_0(D_1^+)$, if and only if D_1^+ is D^+ . To define the discontinuity of f^+ around $L_0(D^+)$ near \bar{p} it is convenient to introduce the local coordinates described at the end of Section II. The Landau surface $L_0(D^+)$ near \bar{p} is then mapped into $\{z_1 = 0\}$, and the physical region $\mathcal{P}(D^+)$ near \bar{p} is mapped into the positive real axis in z_1 space.

The domain of analyticity of $f^+(p(z))$ near $z = z(\bar{p}) = \bar{z} = 0$ is, according to the NAS, controlled by the vectors $u'(D_1^+(\bar{p}))$. In our case there is, modulo dilations, just one such vector,

$$\begin{aligned} u' &= \nabla \phi(p(\bar{z}); D^+(\bar{p})) \\ &= \nabla \bar{z}_1 \\ &= (1, 0, \dots, 0) . \end{aligned}$$

Thus $f^+(p(x))$ at any real point sufficiently near $x = 0$ is the limit of the analytic function $f^+(z) = f^+(p(z))$ from any direction in $y = \text{Im } z$ space that satisfies $y \cdot u' > 0$; i.e., $f^+(p(x))$ near $x = 0$ is essentially the limit of $f^+(p(z))$ from the upper-half z_1 plane.

The discontinuity of f^+ around $L_0(D^+)$ is defined to be f^+ minus the function f' obtained by analytically continuing f^+ from the region $x_1 < 0$ into the region $x_1 > 0$ by a path that passes around $z_1 = 0$ via a detour into the lower half z_1 plane, as indicated in the figure below:

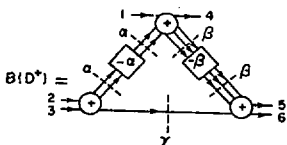


This discontinuity is evidently zero at points $x_1 < 0$.

The general formula for this discontinuity is illustrated by the following example: if



then the discontinuity of f^+ around $L_0(D^+)$ is the function represented by



The letters α , β , and γ label certain specified sets of particles, and the corresponding dotted lines cut sets of internal lines that correspond to these sets of particles. The $-\alpha$ box represents the function S_α^{-1} defined by

$$S_\alpha S_\alpha^{-1} = I_\alpha.$$

where S_α and I_α are the restrictions of S and I to the space corresponding to the set of particles α .

The formula in any other case is constructed analogously: each vertex of D^+ is replaced by a plus bubble, and on each set of lines α connecting a pair of vertices of D^+ there is inserted a $-\alpha$ box.

This formula holds in some small neighborhood of the specified point \bar{p} . Later we shall obtain some discontinuities formulae that hold globally (i.e., at all real points $p \in \mathcal{M}_0^+$). These global formulas are the ones that control the principal contributions to the dispersion relations, but the local ones described above are also important. For example, they are needed in the derivation of the Reggeon discontinuity formulas.

V. DERIVATION OF THE FORMULA FOR THE DISCONTINUITY OF F^+ AROUND $L_0(D^+)$

In this section it is shown how the formula for the discontinuity of F^+ around $L_0(D^+)$ is derived. First the general method is outlined, and then some examples are given.

1. General Method

Consider a diagram D^+ and a point $\bar{p} \in \mathcal{M}^+$ that lies on $L_0(D^+)$ if and only if D_1^+ is D^+ .

Step 1 Use unitarity and the cluster decomposition properties of S and S^+ to effect a decomposition

$$F^+ = T(D^+) + R(D^+) , \quad (1.1)$$

such that

$$T(D^+) = B(T, D^+) \quad (1.2)$$

and

$$R(D^+) = B(R, D^+) . \quad (1.3)$$

The $B(T, D^+)$ and $B(R, D^+)$ are sums of bubble diagrams, each multiplied by a nonzero scalar coefficient. These coefficients are generally plus or minus one, and the sums represent the sums of the corresponding bubble diagram functions, each multiplied by the corresponding scalar coefficient. The following two demands are made:

(a) For each B in $B(T, D^+)$, $D(B)$ contains D^+ . (1.4)

(b) No B in $B(R, D^+)$ supports D^+ . (1.5)

HENRY P. STAPP

B supports D if and only if some D' that fits into B contains D. A diagram D' contains a diagram D if and only if the lines of D can be placed in one-to-one correspondence with a subset of the lines of D', and the contraction to points of the remaining lines of D', all of which must be internal, reduces D' to D. A signed line of D can be placed in correspondence with a line of D' having either the same sign, or having no sign, but not with any line of D' having the opposite sign. The main problem in calculating the discontinuity formula is to find a decomposition satisfying (1.1)-(1.5).

Step 2 Consider first only those singularities that correspond to solutions of the Landau equations in which all α 's are positive or zero, or all α 's are negative or zero; i.e., temporarily ignore all mixed- α singularities, which are singularities corresponding to solutions of the Landau equations in which some α 's are positive and others are negative.

Because \bar{p} lies on $L_0(D^+)$, but on no other basic positive- α surface, all vectors $u(D^+(\bar{p}))$ corresponding to positive- α solutions are positive multiples of $u(D^+(\bar{p}))$, by virtue of Theorem 6, and all vectors $u(D^+(\bar{p}))$ corresponding to negative- α solutions are negative multiples of $u(D^+(\bar{p}))$.

The functions f^+ , $t(D^+)$, and $r(D^+)$ represent the functions F^+ , $T(D^+)$, and $R(D^+)$, with the factor $(2\pi)^4 \delta(x_1)$ removed. The NAS says that $f^+(\bar{p}(x))$, near \bar{p} , is the boundary value of $f^+(\bar{p}(z))$ from within the cone dual to $u(D^+(\bar{p}))$, i.e., essentially from the upper-half z_1 plane.

The analytic structure of $r(D^+)$ is given by the structure theorem. The requirement (b) on $B(R, D^+)$ ensures that none of the singularities of $r(D^+)$ correspond to diagrams that contain D^+ . If mixed- α singularities are ignored this leaves only the singularities corresponding to the negative- α solutions. All the vectors $u'(D^+(\bar{p}))$ corresponding to these negative- α solutions are negative multiples of $u'(D^+(\bar{p}))$. Consequently, $r(D^+)$ is the limit from the lower-half z_1 plane.

Property (a) of $B(T, D^+)$ ensures that $T(D^+)$ vanishes outside $\rho(D^+)$, i.e., in $x_1 < 0$. Thus in this region the function f^+ coincides with $r(D^+)$.

Therefore $r(D^+)$ is a function that coincides with f^+ in the region $x_1 < 0$ (i.e., below the threshold $x_1 = 0$) and that continues around $x_1 = 0$ by a detour into the lower-half z_1 plane. Thus $r(D^+)$ is the function f' of the preceding section, and the difference $f^+ - r(D^+) = t(D^+)$ is the discontinuity.

Step 3 Use the discontinuity formulas obtained, neglecting mixed- α singularities, in steps 1 and 2 to show that all mixed- α singularities in $r(D^+)$ cancel among themselves.

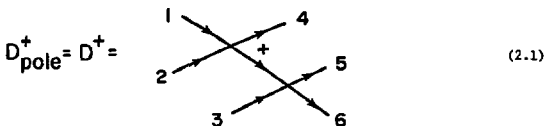
This procedure leads (at least in the formal framework described below) to the unique discontinuity formulas described at the end of the preceding section. However, it is based on the ansatz that the mixed- α singularities cancel among themselves. Hence the possibility of some other solution, in which the mixed- α singularities do not cancel among themselves, is not ruled out.

Derivations not based on the mixed- α cancellation ansatz are blocked, at the present time, by the inadequacy of the structure theorem at $u = 0$ points. If one uses a recently proposed, but still unproved, new version of the structure theorem that does adequately cover $u = 0$ points then it is possible to derive without using the mixed- α cancellation ansatz, and also to prove unique, the discontinuity formula described above at least in the simplest of all cases, which is the pole-factorization theorem below the four-particle threshold in the equal-mass case. However, this new theorem is still unproved and has not been applied to any other cases. Thus we shall use, in the present work, the mixed- α cancellation ansatz, and leave aside the question of uniqueness, except to express the opinion that a consistent solution of the unitarity and analyticity conditions in which the mixed- α do not cancel among themselves is surely impossible.

The third step listed above, namely the verification that all mixed- α singularities do indeed cancel out among themselves in $R(D^+)$ has been carried out in many special cases, but has not been proved in general.

2. Pole-Factorization Theorem Below 4-Particle Threshold

In this special case the diagram D^+ in question is the pole diagram



Unitarity and cluster decomposition give

$$\begin{aligned}
 \Xi^+ - \Xi^- &= \Xi^+ - \Xi^- + \sum_{(3)} \Xi^+ - \Xi^- \\
 &+ \sum_{(3)} \Xi^+ - \Xi^- + \sum_{(9)} \Xi^+ - \Xi^- \\
 \end{aligned} \tag{2.2}$$

where, merely to shorten the formulas, the t -particle intermediate states have been omitted. Postmultiplying (2.2) by

$$\Xi^+ - \Xi^- = \sum_{(3/)} \Xi^+ - \Xi^- + \sum_{(9)} \Xi^+ - \Xi^- \tag{2.3}$$

rearranging terms, and using two-particle unitarity,

$$\begin{aligned}
 \Xi^+ - \Xi^- &= \Xi^+ - \Xi^- \\
 &= \Xi^- - \Xi^+ \\
 \end{aligned} \tag{2.4}$$

one obtains

$$F^+ = T(D^+) - R(D^+) \tag{2.5}$$

where

$$F^+ \sim \Xi^+ \tag{2.6}$$

$$T(D^+) = \text{Diagram 1} + \text{Diagram 2}$$

$$= \text{Diagram 3}$$

(2.7)

and

$$R(D^+) = \sum_{(3)} \text{Diagram 4} + \sum_{(9)} \text{Diagram 5}$$

$$+ \sum_{(8)} \text{Diagram 6}$$

$$+ (\text{Diagram 7} + \text{Diagram 8} + \sum_{(3)} \text{Diagram 9}) \times$$

$$(\sum_{(3!)} \text{Diagram 10} + \sum_{(9)} \text{Diagram 11})$$

(2.8)

Properties (a) and (b) are easily checked:

(a) $B(T, D^+)$ is the right-hand side of (2.7). It consists of a single diagram B , and $D(B)$ clearly contains D^+ .(b) $B(R, D^+)$ is the right-hand side of (2.8). It is easy to see that no B in $B(R, D^+)$ supports D^+ .

The following two observations suffice:

(i) Stability conditions entail that each vertex of a Landau diagram have at least two initial lines and at least two final lines. (The others correspond to empty sets $L(D)$, and are to be omitted.) Thus the two lines coming into a two-to-two bubble must meet at a vertex. This fact, together with the fact that the diagram D_b inserted into each bubble b must be a connected diagram, precludes the possibility of fitting D^+ into any bubble diagram in the first three sums in $R(D^+)$.

(ii) In considering whether a D^+ fits into a B one may consider each minus bubble of B to be a point vertex, since all lines coming from inside such a bubble carry minus signs, and hence must be contracted to points in the contraction that yields D^+ . But the contraction of the big minus bubbles in the remaining term in $R(D^+)$ renders it unable to support D^+ .

Decomposition of Singularities This formula for the discontinuity near \bar{p} ,

$$F^+ - R(D^+) = \text{Diagram with two lines entering a vertex with a plus sign, and two lines leaving a vertex with a plus sign.}$$

together with the NAS, implies that near \bar{p}

$$F^+ \approx \text{Diagram with two lines entering a vertex with a plus sign, and two lines leaving a vertex with a plus sign.}$$

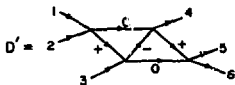
and

$$R(D^+) \approx - \text{Diagram with two lines entering a vertex with a plus sign, and two lines leaving a vertex with a plus sign.}$$

Here \approx means equal in the sense of microfunction (and locally modulo analytic functions), and a plus (or minus) sign on a line L_i of a bubble diagram B means that only those parts of the singularities of F^B that correspond to vectors $u'(D^+(\bar{p}))$ associated with solutions of the Landau equations with $\alpha_i > 0$ (or $\alpha_i < 0$) are accepted. Similarly a zero on a

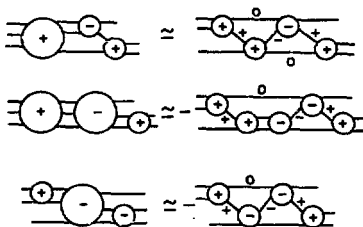
line L_1 of a bubble diagram B means that only those parts of the singularities of F^B that correspond to solutions of Landau equations with $a_1 = 0$ are accepted. The notion of a decomposition of singularities into parts associated with different directions $u(D(\vec{p}))$ is the heart of the theory of essential support, and of the theory of microfunctions. It is closely connected with the local decomposition of $2\pi \delta(p_1^2 - m_1^2)$ into $ic/p_1^2 - m_1^2 + ic$ and $-ic/p_1^2 - m_1^2 - ic$.

Cancellation of Mixed-a Singularities Consider the Landau diagram



where a zero on a line L_1 of a Landau diagram indicates that the corresponding a_1 is zero. The associated Landau surface $L(D')$ is confined to $L_0(D_{pole}^+)$, and may coincide with $L(D_{pole}^+)$ in some neighborhood of \vec{p} . If such a mixed-a singularity were present in $R(D_{pole}^+)$ it would disrupt the derivation of the formula for the discontinuity around $L_0(D_{pole}^+)$.

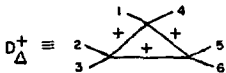
However, the various contributions to $R(D_{pole}^+)$ associated with this diagram D' exactly cancel:



The three bubble diagrams on the left are the only ones in $B(r, D_{pole}^+)$ that support D' . Their contributions to the singularity corresponding to D' are indicated on the right. These contributions sum to zero, by virtue of two-particle unitarity.

3. Triangle Diagram Singularity

(Below the 4-particle threshold). Define



Consider the expansion $F^+ = T^+(D_{\text{pole}}^+) + R(D_{\text{pole}}^+)$ used in the preceding subsection. The only B 's in $B(T, D^+) + B(R, D^+)$ that support D_{Δ}^+ are

$$\begin{aligned}
 & \text{Diagram 1: } + \text{ (a circle with a plus sign and a minus sign on the right)} \\
 & \text{Diagram 2: } - \text{ (a circle with a plus sign and a plus sign on the right)} \\
 & \text{Diagram 3: } + \text{ (a circle with a plus sign and a plus sign on the right)} \\
 & \text{Diagram 4: } - \text{ (a circle with a minus sign and a plus sign on the right)} \\
 & \text{Diagram 5: } (+ \text{ (a circle with a plus sign and a minus sign on the right)} + \text{ (a circle with a plus sign and a plus sign on the right)} + \text{ (a circle with a minus sign and a minus sign on the right)}) \text{ (a circle with a plus sign and a minus sign on the right)} \\
 & \text{Diagram 6: } + \text{ (a circle with a plus sign and a plus sign on the right)} \\
 & \text{Diagram 7: } - \text{ (a circle with a minus sign and a plus sign on the right)} + \sum_{(3)} \text{ (a circle with a plus sign and a minus sign on the right)} \\
 & \text{Diagram 8: } + \sum_{(2)} \text{ (a circle with a plus sign and a minus sign on the right)} + \sum_{(6)} \text{ (a circle with a plus sign and a minus sign on the right)} \text{ (a circle with a plus sign and a minus sign on the right)} \\
 & \text{Diagram 9: } + \text{ (a circle with a plus sign and a plus sign on the right)}
 \end{aligned}$$

Only the last term supports D_{Δ}^+ . And the $D(B)$ corresponding to this last term contains D_{Δ}^+ . Thus if this last term is identified as $T(D_{\Delta}^+)$ then the required conditions (a) and (b) on $T(D_{\Delta}^+)$ and $R(D_{\Delta}^+)$ are satisfied.

4. The Indented Box

Theorem 7 Unitarity and cluster decomposition entail that

$$\alpha \boxed{-} \beta + \gamma \equiv \alpha \boxed{-} \beta + \gamma \quad \alpha \boxed{+} \beta + \gamma$$

(4.1)

where the indented box represents the sum

$$\sum_{n=0}^{\infty} \sum_{\alpha_i, \gamma_i} (-1)^m \alpha_{m+1} \boxed{\alpha_m \dots \alpha_1} \beta + \gamma_1 \quad \alpha_m \dots \alpha_1 \boxed{+ - + - + \dots} \beta + \gamma_2$$

(4.2)

Only a finite number of terms contribute to this sum at any (finite) point p . There is a sum over all ways of decomposing the set α into parts $\alpha_1, \dots, \alpha_{n+1}$, a sum over all ways of decomposing γ into parts γ_1 and γ_2 , and

$$\alpha \boxed{-} \beta + \gamma = \left\{ \begin{array}{l} \text{The sum of all terms in the cluster} \\ \text{decomposition of the box in which each} \\ \text{line of } \alpha \text{ is connected by a bubble to} \\ \text{some line of } \beta. \end{array} \right.$$

(4.3)

Examination of (4.2) shows that the indented box is a sum of bubble diagrams B with the following property: no B in this sum supports any D having a set $\alpha' \neq \alpha$ of positively signed lines which if cut separate the diagram into two parts A and B such that A has incoming lines α and outgoing lines α' and B has incoming lines α' and B and outgoing lines γ . That is, no D that fits into any B in the indented box can be decomposed into a structure of the form



(4.4)

unless $\alpha' \in \alpha$ (i.e., unless A contains only trivial bubbles). The A and B are allowed to be either connected or not connected.

Theorem 7 combined with unitarity gives

(4.5)

These results play a central role in the derivation of general discontinuity formulas, and they will be used in the following subsection.

5. Leading Normal-Threshold Formula

Theorem 8

(5.1)

where the arrow box represents

$$\sum_{n=0}^{\infty} \sum_{\substack{\beta_1 \neq \phi \\ \beta_2 = \beta - \beta_1}} H^n$$

(5.2)

The arrow box is a sum of bubble diagrams B with the following property: every D^+ that fits into any B in this sum has a path that begins in β and ends in α' and consists of segments L_i all of which are directed along the path. Thus no B in this sum supports any diagram D of the form



(5.3)

where the A and B are allowed to be either connected or disconnected.

Defining

$$\boxed{+} \equiv \boxed{+} - \boxed{+}$$

(5.4)

one can write

$$\begin{aligned}
 & \text{Diagram 1: } \text{Diagram A} = \text{Diagram B} \\
 & \text{Diagram 2: } \text{Diagram A} = \text{Diagram C} + \text{Diagram D} - \text{Diagram E} \\
 & \text{Diagram 3: } \text{Diagram A} = \text{Diagram F} + \text{Diagram G} - \text{Diagram H}
 \end{aligned}$$

(5.5)

The second and third terms in the last line of this equation support no normal threshold diagram D_t^+ , which is a diagram D^+ of the form (5.3) with point vertices A and B. The last term does support D_t^+ in general, but not at points \bar{p} that lie on no basic surface except $L_0(D_t^+)$. For the disconnected nature of the boxes on the ends of this term entails that the corresponding function vanish unless the conservation-laws corresponding to the disconnected parts are satisfied, and this entails that \bar{p} lie on $L_0(D^+)$ for a corresponding diagram $D^+ \neq D_t^+$. Thus at points \bar{p} that lie on no basic surface except $L_0(D_t^+)$ we can identify the first term in (5.5) as $T(D_t^+)$: then conditions (a) and (b) are satisfied, and $T(D_t^+)$ is the discontinuity around D_t^+ .

VI. FORMAL METHOD

The procedures used in the preceding section allow the discontinuity formula stated at the end of Section IV to be derived in many cases. However, the question arises whether functions $T(D^+)$ and $R(L^+)$ satisfying the required properties exist for all D^+ with nonempty $L_0(D^+)$, whether these functions are unique (within the framework based on the mixed-a cancellation ansatz), and whether the stated formula holds in all cases. The aim of the present section is to explore these questions, and in particular to:

(a) Prove the existence of $T(D^+)$ and $R(L^+)$

(b) Prove the uniqueness of $T(D^+)$ and $R(D^+)$
 (c) Derive the general formula for $T(D^+)$.

The work in this section is based on infinite series expansions for the quantities of interest. The method is formal in the sense that the question of the convergence of these series is not considered: two functions having the same expansion are called equivalent, and are considered to be equal, and analytic properties that hold for every term of an expansion are assumed to hold also for the sum. Also, the mixed-a cancellation ansatz is accepted. Within these limitations the formal method used in this section is neat and powerful.

1. The Minus-Bubble Expansion of S

Write

$$S = S^+ = (I + R^+) \quad (1.1)$$

and

$$S^- = S^- = (I - R^-) . \quad (1.2)$$

Then unitarity,

$$S^- S^+ = I , \quad (1.3)$$

can be written

$$R^+ = R^-(I + R^+) . \quad (1.4)$$

Iteration gives, formally,

$$R^+ = \sum_{n=1}^{\infty} (R^-)^n . \quad (1.5)$$

Theorem 9

$$S = \sum_i B_i^- . \quad (1.6)$$

The sum runs over every bubble diagram B_i^- each bubble of which is a minus bubble, and the convention in which the minus bubble represents $-S_c$ is used.

Theorem 9 follows from (1.5) after some cancellations. For example, the bubble diagram

$$B_i^- = \begin{array}{c} \text{---} \\ \text{---} \end{array} \text{---} \text{---}$$

occurs in three terms of (1.5):

$$+ \begin{array}{|c|c|c|c|} \hline \text{circle} & \text{circle} & \text{circle} & \text{circle} \\ \hline \text{line} & \text{line} & \text{line} & \text{line} \\ \hline \end{array} + \begin{array}{|c|c|c|c|} \hline \text{circle} & \text{circle} & \text{circle} & \text{circle} \\ \hline \text{line} & \text{line} & \text{line} & \text{line} \\ \hline \end{array} - \begin{array}{|c|c|c|c|} \hline \text{circle} & \text{circle} & \text{circle} & \text{circle} \\ \hline \text{line} & \text{line} & \text{line} & \text{line} \\ \hline \end{array}$$

The first two terms come from $(\bar{R})^2$, whereas the last comes from \bar{R} . The minus sign in the last term comes from the one minus sign in (1.2) and two minus signs from the minus bubble convention.

Corollary

$$S_c = \sum_c B_i^- \quad (1.7)$$

where S_c is the connected part of S , and the sum runs over the connected B_i^- .

2. Formal Framework

Any B can be expressed in a unique way as a linear combination of the various minus bubble diagrams B_i^- : one simply replaces each plus bubble b^+ of B by its expansion (1.7) and collects terms. This gives

$$B = \sum_i n_i(B) B_i^- , \quad (2.1)$$

where the sum runs over the set of all bubble diagrams B_i^- having only minus bubbles. The infinite set of numbers $n_i(B)$ is regarded as an infinite dimensional vector $n(B)$, and all B having the same $n(B)$ are said to be equivalent. Sums $B = \sum_i c_i B_i^-$ of bubble diagrams B_i^- with scalar coefficients c_i can also be considered, and the corresponding vector $n(B)$ is defined to be $\sum_i c_i n(B_i^-)$. By this procedure the B_i^- become the basis vectors of a linear space of (generalized) bubble diagrams B .

Theorem 10 If B_1^- can be transformed into B_2^- by an application of unitarity and cluster decomposition then B_1^- is equivalent to B_2^- .

Outline of Proof The unitarity equations,

$$S^+ S^- - I = 0 , \quad (2.2)$$

are equivalent to zero:

$$n \left[\begin{array}{|c|c|c|c|} \hline \text{circle} & \text{circle} & \text{circle} & \text{circle} \\ \hline \text{line} & \text{line} & \text{line} & \text{line} \\ \hline \end{array} + \begin{array}{|c|c|c|c|} \hline \text{circle} & \text{circle} & \text{circle} & \text{circle} \\ \hline \text{line} & \text{line} & \text{line} & \text{line} \\ \hline \end{array} - \begin{array}{|c|c|c|c|} \hline \text{circle} & \text{circle} & \text{circle} & \text{circle} \\ \hline \text{line} & \text{line} & \text{line} & \text{line} \\ \hline \end{array} - I \right] = 0 \quad (2.3)$$

For example, in the two-to-two case

$$\text{Diagram with a plus sign} = I + \sum_{n=1}^{\infty} (\text{Diagram with a minus sign})^n \quad (2.4)$$

and

$$\text{Diagram with a minus sign} = I - \text{Diagram with a minus sign} \quad (2.5)$$

Multiplying (2.4) by (2.5) and collecting terms one finds that every term but I drops out. Thus (2.3) holds in this case. In fact, it holds in general: i.e., in the expansion of (2.2) in terms of minus bubble diagrams B_1^- , each B_1^- occurs with net coefficient zero.

In any application of unitarity and cluster decomposition one replaces some B_1 by B_2 where B_1 and B_2 differ by parts B_1' and B_2' that are equal by virtue of unitarity and cluster decomposition. These two parts are therefore equivalent, by virtue of (2.3): the expansion of B_1' in terms of minus bubbles is identical to the expansion of B_2' . But then the replacement of B_1' by B_2' in B will not alter the minus bubble expansion of the larger diagram: B_1 will be equivalent to B_2 .

Theorem 10 is the basis of the usefulness of the representation $n(B)$ of B : this representation is invariant under the operations of applying unitarity and cluster decomposition. Any two B 's that are equal by virtue of unitarity and cluster decomposition, are represented by the same vector $n(B)$, and conversely, any two B 's that are equivalent can be formally converted to the same infinite series by using unitarity and cluster decomposition, and this infinite series, which is specified by $n(B)$, is moreover unique.

3. Existence of $T(D^+)$ and $R(D^+)$

Let $B^-(T, D^+)$ be the sum of all connected B_1^- that support D^+ . Let $B^-(R, D^+)$ be the sum of all connected B_1^- that do not support D^+ . Let $B^-(F^+)$ be the sum of all connected B_1^- . Then

$$B^-(F^+) = B^-(T, D^+) + B^-(R, D^+) . \quad (3.1)$$

The corollary of Theorem 9 says that $B^-(F^+)$ is equivalent to F^+ :

$$B^-(F^+) = F^+ . \quad (3.2)$$

The sum $B^-(R, D^+)$ satisfies the defining property of $B(R, D^+)$. Moreover, the sum $B^-(T, D^+)$ satisfies the defining property of $B(T, D^+)$, by virtue of the following equivalence: for any bubble diagram B^- each bubble of which is a minus bubble

$$B^- \text{ supports } D^+ \text{ if and only if } D(B^-) \text{ contains } D^+. \quad (3.3)$$

This is true because every positively signed line in any D that fits into B^- is a line of $D(B^-)$, and conversely $D(B^-)$ fits into B^- .

Since the requirements on the various terms are all satisfied (3.1) is a formal solution of the equation

$$F^+ = T(D^+) + R(D^+). \quad (3.4)$$

The general formula for $T(D^+)$ given in Section IV is the result of reassembling the infinite set of terms in $B^-(T, D^+)$ into an equivalent finite expression $B(T, D^+)$, as will be shown later.

4. Uniqueness of the $T(D^+)$ and $R(D^+)$

Theorem 11 Let

$$F^+ = B^-(T, D^+) + B(R, D^+) \quad (4.1)$$

be any decomposition of F^+ that is derived solely from unitarity and cluster decomposition and that satisfies the defining conditions for $B(T, D^+)$ and $B(R, D^+)$. Then the following equivalences hold:

$$B(T, D^+) = B^-(T, D^+) \quad (4.2)$$

and

$$B(R, D^+) = B^-(R, D^+). \quad (4.3)$$

Proof Suppose B is in $B(T, D^+)$. Then $D(B)$ must contain D^+ . But the procedure that converts B into its image B' in the space of B_i^- leaves unchanged every line of $D(B)$: i.e., B' contains $D(B)$, and hence D^+ . Thus every B_i^- in $B'(T, D^+)$ contains D^+ , and hence belongs to $B^-(T, D^+)$:

$$\{n_i(B(T, D^+)) \neq 0\} \implies \{n_i(B^-(T, D^+)) = 1\}. \quad (4.4)$$

Suppose B is in $B(R, D^+)$. Then, by definition, no D that fits into B contains D^+ . But the procedure that converts B to its image B' in the space of B_i^- introduces no plus lines that are not present in some D that fits into B . Thus no B_i^- in $B'(R, D^+)$ can support D^+ :

$$\{n_i(B(R, D^+)) \neq 0\} \implies \{n_i(B^-(R, D^+)) = 1\}. \quad (4.5)$$

On the other hand, Eq. (4.1) is derived solely from unitarity and cluster decomposition. Thus the two sides are equivalent, and hence for every i

$$n_i(B(T, D^+)) + n_i(B(R, D^+)) = 1. \quad (4.6)$$

Since the sets

$$(i: n_1(B^-(T, D^+)) = 1)$$

and

$$(i: n_1(B^-(R, D^+)) = 1)$$

are disjoint, by construction, the conditions (4.4), (4.5), and (4.6) imply that for all i

$$n_1(B(T, D^+)) = n_1(B^-(T, D^+)) \quad (4.7)$$

and

$$n_1(B(R, D^+)) = n_1(B^-(R, D^+)). \quad (4.8)$$

These are the desired conditions (4.2) and (4.3).

The decomposition (4.1) therefore exists and is unique, within the formal framework. The remaining problem is to show that the discontinuity formula given at the end of Section IV is equivalent to $B^-(T, D^+)$, near points p lying on $L_0(D_1^+)$ if and only if D_1^+ is D^+ .

5. The Indented Box Revisited

To introduce some ideas needed for the derivation of the general discontinuity formula we consider again the formula

$$\alpha \xrightarrow{\beta} \begin{matrix} - \\ + \end{matrix} \gamma = \alpha \xrightarrow{\beta} \begin{matrix} - \\ + \end{matrix} \gamma \quad (5.1)$$

Definition A bubble whose initial lines consist exclusively of lines from the set α is called an α bubble.

Definition

$$S'(\underline{\alpha}, \underline{\beta}; \gamma) \equiv \alpha \xrightarrow{\beta} \begin{matrix} / \\ + \end{matrix} \gamma \quad (5.2)$$

is the sum of all B_1^- that have incoming lines α and β , outgoing lines γ , but have no α bubble. It is called $S(\alpha, \beta; \gamma)$ truncated on α .

Remark Each term of $S'(\underline{\alpha}, \underline{\beta}; \gamma)$ satisfies the characteristic property of the indented box, which is that no $\alpha' \neq \alpha$ effects a separation of the form of (4.4) of Section V. And every B_1^- not in $S'(\underline{\alpha}, \underline{\beta}; \gamma)$ fails to satisfy this characteristic property.

Theorem 12

$$\begin{array}{c} \alpha = \square - \square \\ \beta = \square + \square \end{array} \quad \gamma = \begin{array}{c} \alpha \quad \square - \square \\ \beta \quad \square + \square \end{array}' = \gamma \quad (5.3)$$

Proof Map the left-hand side into B_1^- space by inserting the expansion S' of S given in (1.6):

$$\begin{array}{c} \alpha \quad \square - \square \\ \beta \quad \square + \square \end{array} = \gamma \simeq \begin{array}{c} \alpha \quad \square - \square \\ \beta \quad \square + \square \end{array}' = \gamma \quad (5.4a)$$

$$= \begin{array}{c} \alpha \quad \square' \\ \beta \quad \square + \square \end{array} + \begin{array}{c} \alpha \quad \square - \square \\ \beta \quad \square + \square \end{array}' = \gamma \quad (5.4b)$$

where

$$\begin{array}{c} \square - \square \\ \square + \square \end{array} = \begin{array}{c} \square - \square \\ \square \end{array} - \begin{array}{c} \square \\ \square \end{array} \quad (5.5)$$

Consider a B_1^- with exactly one α bubble. It occurs exactly once in the first term of (5.4b) (i.e., in S'), and with a plus sign. It also occurs exactly once in the second term, in the diagram obtained by shifting this one α bubble into the slashed minus box. In this term it occurs with a minus sign (we are using the convention where the minus bubble represents $-S_c$). Thus the two terms cancel. If B_1^- has n α bubbles then there are, in an exactly similar way, 2^n terms in (5.4b) that exactly cancel out. But if B_1^- has no α bubble then B_1^- occurs in S' but not in the second term, and there is no cancellation. This gives (5.3).

6. Flowlines and Schnitts

To prove general discontinuity formulas the concepts of flow lines and schnitts are useful. A flowline is a path in a Landau diagram D that runs from the extreme left of the diagram to the extreme right. It consists of an ordered sequence of line segments L_i of D all of which point in the direction of the path. A schnitt α is a cutting of a set of lines L_i of a diagram. It is allowed to cut no flow line more than once. The set f_α is the set of flow lines cut by α . Equivalent schnitts α are schnitts that cut the same set of flow lines. A line L_1 lies right (resp. left) of line L_2 if and only if L_1 lies right (resp. left) of L_2 on some flow line. A schnitt α_1 lies right (resp. left) of a schnitt α_2 if and only if α_1 is equivalent to α_2 and some line L_1 cut by α_1 lies right (resp. left) of some line L_j cut by α_2 , and no line L_1 cut by α_1 lies left (resp. right) of any line L_j cut by α_2 . A rightmost

(resp. leftmost) schnitt α is a schnitt such that no schnitt α' lies right (resp. left) of it. The rightmost (resp. leftmost) schnitt equivalent to any given schnitt is well defined.

A schnitt in a bubble diagram B is a schnitt in $D(B)$.

Consider now the set of B_i^- that have initial lines α and β and final lines γ . The sets α and β define leftmost schnitts, and γ defines a rightmost schnitt. Let α' be the rightmost schnitt equivalent to α . The sum of all these diagrams is represented by

$$\alpha \text{---} \boxed{+} \text{---} \gamma = \alpha \text{---} \boxed{+} \text{---} \overset{1}{\alpha'} \text{---} \boxed{+} \text{---} \beta \text{---} \boxed{+} \text{---} \gamma,$$

(6.1)

where the primed boxes represent the expansions of the unprimed boxes in terms of the B_i^- . The identity (6.1) follows from the fact that the schnitt α' has a well-defined location in each B_i^- , and hence one gets each term on the left-hand side once and only once by combining independently the sum of all B_i^- that can occur on the right of α' , which is the sum that represents $S(\alpha, \beta; \gamma)$ truncated on α , with the sum of all possible B_i^- that can occur on the left of α' , which is the sum of all B_i^- that represent $S(\alpha; \alpha')$. This argument will be used several times in what follows.

Application of unitarity to (6.1) give a (5.1).

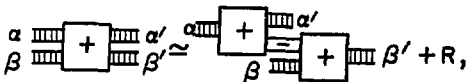
Consider next the set of all B_i^- that have incoming sets α and β and outgoing sets α' and β' . Separate these B_i^- into two sets. The first set consists of those that have a schnitt γ such that (1) all flow lines in γ start in α and end in β' , and (2) the schnitt γ cuts B_i^- into two disjoint parts one containing γ and γ' the other containing β and β' . The second set is the remainder R .

Let γ' be the rightmost schnitt equivalent to γ . Then the sum of these diagram B_i^- can be collected into the expression

$$\alpha \text{---} \boxed{+} \text{---} \overset{1}{\alpha'} \text{---} \beta' = \alpha \text{---} \boxed{+} \text{---} \overset{1}{\alpha'} \text{---} \gamma' \text{---} \boxed{+} \text{---} \beta' + R,$$

(6.3)

This result combined with (5.3) gives,



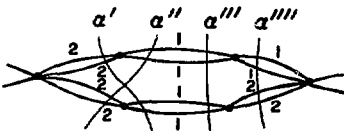
(6.4)

from which the normal-threshold discontinuity formula can be derived as before.

7. Strongly Equivalent Schnitts

The mass of a schnitt is the sum of the masses of the lines cut by the schnitt. Two schnitts are strongly equivalent if and only if they are equivalent and have the same mass.

The concept of the rightmost (or leftmost) schnitt strongly equivalent to given schnitt is not always well defined. For example, if the masses m_1 and m_2 satisfy $m_1 > m_2$ then in



the two schnitts a' and a'' are both strongly equivalent to a , but there is no unique leftmost schnitt strongly equivalent to a . However, a simple argument shows that there will always be a unique leftmost (and rightmost) schnitt a' strongly equivalent to any given schnitt a if there is no schnitt a'' equivalent to a but with larger mass.

Consider the set or all \bar{B}_1 with incoming lines a and β , and outgoing lines γ . Let $\bar{p} \in \mathcal{M}_1^r$ be a point such that all of the \bar{p}_j in a are parallel. Let $X(\bar{p})$ be the subspace generated by the set of all \bar{B}_1 such that \bar{p} lies outside $\mathcal{P}(\bar{B}_1)$. Then

$$\begin{array}{c} a \\ \beta \end{array} \begin{array}{c} + \\ \end{array} \begin{array}{c} 1 \\ \gamma \end{array} = \begin{array}{c} a \\ \beta \end{array} \begin{array}{c} + \\ \end{array} \begin{array}{c} 1 \\ a \\ + \\ \gamma \end{array} \mod X(\bar{p}).$$

(7.1)

The condition $\mod X(\bar{p})$ means modulo contributions corresponding to B_i^- in $X(\bar{p})$. All contributions B_i^- in which there is a schmitt a'' that is equivalent to a but with larger mass fall into this class. When these B_i^- are excluded the rightmost schmitt a' strongly equivalent to a is well defined. Every term of the remaining sum of B_i^- appears exactly once in the box expression on the right-hand side of (7.1)

8. Nonleading Normal Threshold

A slight modification of the argument leading to (6.3) gives this same formula with γ' now the rightmost schmitt strongly equivalent to a schmitt γ of some definite mass M_γ , and R expanded to include terms B_i^- that have schmitts equivalent to γ but with larger mass. Then from (7.1) one obtains

$$\begin{array}{c} a \\ \beta \end{array} \begin{array}{c} + \\ \end{array} \begin{array}{c} a' \\ \gamma' \end{array} \simeq \begin{array}{c} a \\ \beta \end{array} \begin{array}{c} + \\ \gamma \\ + \\ \beta' \end{array} + R',$$

(8.1)

where the $-\gamma$ box represents the inverse S_γ^{-1} of the restriction S_γ of S to γ space, which is the sum of the spaces corresponding to all sets of particles the sum of whose masses is the same as that of the set γ . From this formula (8.1) one derives the discontinuity around a nonleading normal threshold by the procedure of Section V.6.

9. Truncated Scattering Functions

Let a and β represent the initial and final variables of a scattering function:

$$a = (p_1, \dots, p_m) \quad (9.1)$$

$$\beta = (p_{m+1}, \dots, p_n) .$$

Let some subset of the set a be separated into a set of disjoint sets a_1, \dots, a_s . Recall that $S_c(a; B) = F^+(a; B)$ is equivalent to the sum of all connected B_i^- . The function F^+ truncated on a_i is defined to be the sum of all connected B_i^- that have no a_i bubble, i.e., that have no bubble each initial line of which corresponds to a variable in a_i . Similarly, the function F^+ truncated on several sets a_i is the sum of all connected B_i^- having no a_i bubble for any a_i in this set. The function F^+ truncated on the set a_1, \dots, a_s of sets a_i is represented by

$$\prod_{i=1}^s \Gamma_{a_i} F^+ .$$

Lemma 1 Let a_1, \dots, a_s be a decomposition of a subset of the set of variables a . Let \bar{p} be a point such that for each $i = 1, \dots, s$ all the \bar{p}_j in a_i are parallel. Then \bar{p} will lie on various Landau surfaces corresponding to diagrams in which there is for each a_i , considered as a schnitt, a rightmost schnitt a'_i strongly equivalent to it, and all of the lines cut by all of these schnitts a'_i terminate on one single vertex. Suppose \bar{p} lies on no positive- a Landau surface corresponding to a diagram in which these lines terminate on more than one vertex. Then

$$F^+(a; B) = \int \prod_{i=1}^s [S(a_i; a'_i) da'_i \Gamma_{a_i}] F^+(a'_1, \dots, a'_s, a_s; B) \bmod X(\bar{p}) . \quad (9.2)$$

where the integral over a'_i is over all sets of variables the sum of whose masses is the same as that of a_i , and $X(\bar{p})$ is the linear space generated by those B_i^- that satisfy $\bar{p} \notin \partial(B_i^-)$.

Proof The left-hand side of (9.2) is equivalent to the sum over all connected B_i^- . The mod $X(\bar{p})$ condition allows us to ignore, as above, all contributions B_i^- in which any a_i (considered as a schnitt) is equivalent to a schnitt of greater mass. Then for any one of the remaining B_i^- one can consider, for each a_i , the rightmost schnitt a'_i strongly equivalent to a_i . Consider next the part P' of this B_i^- that lies to the right of all of the rightmost schnitts a'_i . This part P' is either connected or is not connected. If it is not connected then B_i^- lies in $X(\bar{p})$. For if \bar{p} lies in $\partial(B_i^-)$ then the conservation-law constraints corresponding to the various disconnected parts of P' must be satisfied, and \bar{p} must consequently lie on one of the Landau surfaces excluded by the hypothesis of the lemma, namely the one in which the lines cut by the rightmost schnitts a'_i terminate, not on one single vertex, but rather on the several vertices corresponding to the several disconnected parts of P' . These B_i^- with disconnected P' may, therefore, also be ignored, due to the mod $X(\bar{p})$ condition, and one is left with the B_i^- such that P' is connected.

The remaining set of B_i^- is generated by summing independently over all possible parts lying on the various sides of the rightmost schnitts a_i' . The part P' lying to the right of all these schnitts a_i' will be just the truncated function occurring in (9.2): i.e., it is the sum of all connected B_i^- that have no a_i bubble for any a_i . And the part lying to the left of the rightmost schnitt a_i' is just the expansion of $S(a_i, a_i')$. Any B_i^- constructed in this way is one of the remaining B_i^- defined above, and each such B_i^- is different because the location of each schnitt a_i' is uniquely defined in each of these remaining B_i^- . Finally, every one of the remaining B_i^- is obtained at least once because every possible combination of parts on the various sides of the various schnitts a_i' is included. Thus the lemma is proved.

The B_i^- that were ignored during proof because they belong to $X(\bar{p})$ satisfy a certain finite set of mass-shell or conservation-law conditions that force \bar{p} to lie outside $\mathcal{P}(B_i^-)$. Thus Eq. (9.2) holds mod $X(p)$ for all p in some finite neighborhood of \bar{p} .

From (9.2) one obtains by inversion, near p ,

$$\sum_{i=1}^s S_{a_i}^{-1} F^+ = \sum_{i=1}^s I_{a_i} F^+ \quad (9.3)$$

where $S_{a_i}^{-1}$ is the inverse of the restriction S_{a_i} of S to the space a_i , which is the sum of the spaces associated with the sets of variables a_i' having sums of rest masses equal to that of a_i .

The function $S_{a_i}^{-1}$ is defined formally by

$$S_{a_i}^{-1} = I_{a_i} + \sum_{n=1}^{\infty} (-R_{a_i})^n \quad (9.4)$$

where I_{a_i} is the restriction of unity to the space a_i and

$$R_{a_i} \equiv S_{a_i} - I_{a_i} . \quad (9.5)$$

10. The General Formula

Theorem 13 For any D^+ let $\Delta(D^+)$ be the discontinuity formula defined at the end of Section IV. Let $\bar{p} \in \mathcal{P}^+$ be a point that lies on $L_0(D^+)$ if and only if D^+ is D^+ . Then

$$\Delta(D^+) = B^-(T, D^+) \bmod X(\bar{p}) \quad (10.1)$$

where $B^-(T, D^+)$ is the sum of all B_i^- that support D^+ , and $X(\bar{p})$ is the subspace generated by the set of B_i^- such that \bar{p} lies outside $\mathcal{P}(B_i^-)$. If for some of the sets of lines of D^+ that run between pairs of vertices of D^+ there are other sets with the same sum of rest masses, so that the theorem as stated above is empty, then D^+ can be interpreted in an expanded sense, in

which each of these sets of intermediate lines is interpreted as a sum over all sets having the same sum of rest masses. The formulas for $\Delta(D^+)$ and $B^-(T, D^+)$ should then also be interpreted in this extended sense: the intermediate sets a'_i should be allowed to run over the other sets with the same sum of rest masses.

Proof Let B_i^- be any diagram in $B^-(T, D^+)$. This diagram supports D^+ . That means that there is a set \mathcal{S} of schnitts a_j of B_i^- whose elements are in one-to-one correspondence with the sets of intermediate lines of D^+ . If for any one of these schnitts there is an equivalent schnitt of greater mass, then \bar{p} lies outside $\mathcal{P}(B_i^-)$ and this B_i^- lies in $X(\bar{p})$, and hence does not contribute to (10.1). For each remaining B_i^- there is for any schnitt in \mathcal{S} a unique rightmost schnitt strongly equivalent to it.

Consider any one of the remaining B_i^- . Let each schnitt a_i in \mathcal{S} be shifted to its rightmost strongly equivalent position a'_i . Let P be the part of B_i^- corresponding to some vertex of D^+ ; it lies to the right of certain schnitts and to the left of others. Consider what happens to P , and to its boundary schnitts, when each a_i is shifted to its rightmost strongly equivalent position a'_i .

One of several things can happen. The first possibility is that the topology is unaffected: i.e., that the new schnitts a'_i lie in the same positions relative to each other as the original schnitts a_i , and that the new part P' is connected. The second possibility is that the new schnitts a'_i lie in the same positions relative to each other as the original schnitts, but that P' is disconnected. In this second case B_i^- belongs to $X(\bar{p})$. For if \bar{p} lies in $\mathcal{P}(B_i^-)$ then it must also lie on $L_0(D''^+)$ for some $D''^+ \neq D^+$; contrary to hypothesis. In particular, it lies on the Landau surface $L(D''^+)$, where D''^+ is the diagram constructed from D^+ by replacing the schnitts bounding P by the schnitts bounding P' , and then joining the lines cut by these new schnitts to vertices corresponding to the various disconnected parts of P' to which they are attached. This surface $L(D''^+)$ is defined by essentially the same conditions that define $L(D^+)$, plus the extra conservation-law conditions entailed by the break-up of the connected part P into the disconnected part P' . But if \bar{p} lies in $\mathcal{P}(B_i^-)$ then these extra conservation-law conditions must be satisfied, and hence \bar{p} must lie in $L(D''^+)$. However, $L(D''^+)$ is the union of $L_0(D''^+)$ with the various surfaces $L_0(D_i''^+)$, where the $D_i''^+$ are certain contractions of D''^+ . Hence \bar{p} must lie on $L_0(D''^+)$ for some D''^+ different from D^+ , contrary to the hypothesis of the theorem. This is not allowed. Thus we conclude that \bar{p} does not lie in $\mathcal{P}(B_i^-)$; i.e., that B_i^- lies in $X(\bar{p})$, and hence does not contribute to (10.1).

The third and final possibility is that the rightmost schnitts a'_1 do not lie in the same position relative to each other as the original schnitts a_1 . Then for some schnitt a_1 standing to the left of some a_j in the original D^+ the rightmost a'_1 strongly equivalent to a_1 lies partly on the right of a'_j . Then some set of flow lines f has a part Q that starts on a subset Q_j of a'_j and ends on a subset Q_1 of a'_1 . The sum of the masses of Q_1 cannot be equal to the sum of the masses of Q_j , for if these sums were equal then a'_j could be moved further right. On the other hand, if the first sum were greater than the second sum then there would be a schnitt a''_j equivalent to a_1 , but having greater mass. If the first sum were less than the second sum then the analogous result is true with a_1 replacing a_j . In either case B_1^- lies in $X(p)$, and does not contribute to (10.1). Thus we are left with the first case; i.e., with the sum of all B_1^- having the following properties: (1) there is a set \mathcal{S} of schnitts a'_1 that separate B_1^- in the manner described by D^+ , (2) for each a'_1 in \mathcal{S} there is no a'_1 equivalent to a'_1 and having greater mass, and (3) when the a'_1 are pushed to their rightmost strongly equivalent positions a'_1 the new parts P' are well defined and connected.

Since the locations of the rightmost schnitts a'_1 in each of the remaining B_1^- are well defined the full sum can be constructed by adding independently all possible contributions corresponding to each of the connected parts P' . The sum of all possible contributions corresponding to any P' is precisely the corresponding function F^+ truncated on those sets of initial variables a_1 that belong to \mathcal{S} . Use of (9.3) converts this form to $\Delta(D^+)$.

The formula (10.1) converts the expression $B^-(T, D^+)$ for the discontinuity $T(D^+)$ obtained in subsections 3 and 4 to the formula quoted at the end of Section IV. The contributions $B_1^- \in X(\bar{p})$ that were ignored in the course of the proof all vanish in some finite neighborhood of \bar{p} .

VII. BASIC DISCONTINUITIES FOR 6-PARTICLE PROCESSES

The discontinuity formulas derived above are local formulas; they give the difference $f^+ - f'$ in some small neighborhood of the point \bar{p} on $L_0(D^+)$. Moreover, this point \bar{p} must lie in $\mathcal{M}' = \mathcal{M}^F - \mathcal{M}_0$.

For dispersion relations one needs global formulas; i.e., formulas that hold at all real points p . And the needed discontinuities are around the leading normal threshold cuts, which always extend to points p lying in \mathcal{M}_0 . Furthermore, one needs not only single discontinuities, but also multiple discontinuities.

Multiple discontinuities across sets of leading normal threshold cuts play a basic role in S-matrix theory and are called basic discontinuities.

Global formulas for all basic discontinuities of six-particle processes have

been derived, and will now be discussed. The derivation has three parts. The first part, which is described in this section, specifies the relevant functions and describes the discontinuities and multiple discontinuities formed from them. The second part, which is described in the next section, proves the analytic structure of these functions at real points $p \in \gamma$. The third, which is described in Section IX, shows that these functions are the appropriate boundary values of a single analytic function; i.e., that there are paths of continuation in the complex mass shell that connect these functions to each other, and that these functions are the boundary values needed for dispersion relations.

Anticipating the later results we shall already in this section refer to certain functions as boundary values from specified sides of various normal threshold cuts. The discontinuities in the three-to-three physical region are discussed first; those in the two-to-four and four-to-two physical regions will be discussed later.

1. The Sixteen Channels g

A channel is defined by a separation of the initial and final lines of a bubble diagram into two disjoint parts, each containing at least two initial lines or at least two final lines. For a three-to-three process the sixteen channels are indicated below



$$g = t$$

$$J_t \equiv \{4,5,6\}$$



$$g = i = 1, 2, \text{ or } 3$$

$$J_i = \{4,5,6,b\}$$



$$g = f = 4, 5, \text{ or } 6$$

$$J_f = \{4,5,6\} - \{f\}$$



$$g = (if)$$

$$J_{(if)} = \{4,5,6,1i - \{f\}\}$$

2. The Sixteen Basic Cuts C_g

Define the invariants

$$s_g \equiv s(J_g) \equiv \left(\sum_{j \in J_g} p_j \right)^2 \quad (2.1)$$

and the cuts

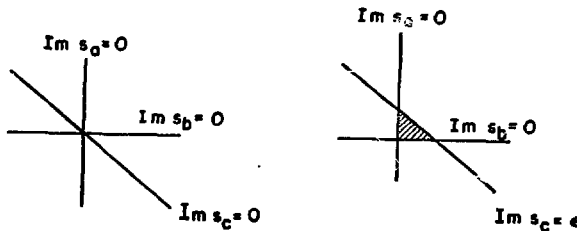
$$C_g \equiv \{p + iq: \operatorname{Im} s_g = 0, \operatorname{Re} s_g \geq s_g^0\}, \quad (2.2)$$

where $s_g^0 = 0$ is the leading normal threshold singularity in channel g ; i.e., s_g^0 is the square of the smallest sum of rest masses of sets of particles that communicate with particles of channel g .

3. The 2^{16} Functions M^G

Let G be any subset of the complete set E of sixteen channel labels g . There are 2^{16} different G 's. For each one we define a function M^G which will be called the boundary value from beneath every cut C_g with $g \in G$ and from above each of the remaining cuts.

The sixteen variable s_g are not all independent. Consequently there are sets G such that there is no mass shell point $(p + iq)$ that lies simultaneously in the lower-half plane $\operatorname{Im} s_g < 0$ for all $g \in G$ and in the upper-half plane $\operatorname{Im} s_g > 0$ for all $g \in \bar{E} = E - G$. For example, if $s_a + s_b = s_c + \text{real const.}$ then it is not possible to have $\operatorname{Im} s_a > 0$, $\operatorname{Im} s_b > 0$ and $\operatorname{Im} s_c < 0$.



However, the cut $\operatorname{Im} s_c = 0$ can in general be pushed back to expose a region of analyticity that lies on top of the cuts $\operatorname{Im} s_a = 0$ and $\operatorname{Im} s_b = 0$ but lies below the displaced cut $\operatorname{Im} s_c = \epsilon$. Boundaries that can be reached only by pushing back some cut in this way are called inaccessible boundaries. The boundary values at both accessible and inaccessible boundaries will be used in the dispersion relations.

4. The 2^{17} Functions T^G and T_G

The functions M^G are defined in terms of some closely related functions T^G

and T_G . These later functions, and also the M^G 's, are defined without reference to the infinite series expansion used in the formal method. And the proofs of the analyticity properties of these functions can be carried out by lattice methods. However, it is useful to present first the infinite series representations of the functions T_G and T^G .

Let D_g^+ be the connected positive diagram that has precisely two vertices, each connected to one of the two sets of lines that define channel g . Then

$$T_g = T = F^+ = \sum_{B_1 \text{ connected}} B_1^-$$

$$T_g = \sum_{B_1 \text{ connected and supports } D_g^+} B_1^-$$

$$T_{gh} = \sum_{B_1 \text{ connected and supports } D_g^+ \text{ and } D_h^+} B_1^-$$

⋮

$$T_G = \sum_{B_1 \text{ connected and supports } D_g^+ \text{ for all } g \text{ in } G} B_1^- \quad (4.1)$$

$$T^0 = T$$

$$T^g = T - T_g$$

$$T^{gh} = T - T_g - T_h + T_{gh}$$

⋮

$$T^G = \sum_{H \subset G} (-1)^{n(H)} T_H \quad (4.2)$$

where $n(H)$ is the number of elements of H .

These definitions entail also

$$T^g = \sum_{B_1 \text{ connected and does not support } D_g^+} B_1^-$$

$$T^{gh} = \sum_{B_1 \text{ connected and supports neither } D_g^+ \text{ nor } D_h^+} B_1^-$$

⋮

$$T^G = \sum_{B_1 \text{ connected and supports no } D_g^+, g \in G} B_1^- \quad (4.3)$$

These properties (4.3) and the structure theorem entail that T^G has no

singularity associated with any diagram that contains D_g^+ for any $g \in G$. Thus it should continue underneath the normal threshold singularities in each channel $g \in G$. On the other hand, (4.2) can be inverted to give

$$T_H = \sum_{G \in H} (-1)^n(G) T^G , \quad (4.4)$$

which is the formula for the multiple discontinuity across the set of cuts H . For example,

$$T_h = T - T^h$$

$$\begin{aligned} T_{hg} &= T - T^h - T^g + T^{hg} \\ &= T - T^h - (T^g - T^{gh}) \end{aligned}$$

etc.

Properties (4.1) ensure that the multiple discontinuity T_H vanishes, as it should, at any real p such that $s_h(p) < s_h^0$ for some $h \in H$.

The general defining properties of the T^G and T_G are:

Property 1

Each T^G can be written as

$$T^G = \sum (-1)^n(H) T_H \quad (4.5)$$

with

$$T_H = \sum_{B \in \mathcal{B}_H} B , \quad (4.6)$$

where for each $B \in \mathcal{B}_H$, and each $h \in H$, $D(B)$ contains D_h^+ .

Property 2

Each T^G can be converted solely by means of unitarity and cluster decomposition properties to a form

$$T^G = \sum_{B \in \mathcal{B}^G} B \quad (4.7)$$

where no B in \mathcal{B}^G supports D_g^+ for any $g \in G$.

Property 3

$$T_g = T^0 = T = F^+ .$$

Property 1 ensures that the multiple discontinuities T_H have the correct support property: they vanish at real p in $s_h < s_h^0$, $h \in H$. Property 2 ensures that T^G continues underneath all normal threshold singularities in channels $g \in G$. Property 3 ensures that T^0 is the physical scattering function F^+ .

A set of functions satisfying these properties 1, 2, and 3 has been constructed by finite methods. The infinite series representations defined in (4.1)-(4.4) formally satisfy these properties, and this solution can be shown to be unique, in the formal framework.

5. The z^{17} Functions \bar{T}^G and \bar{T}_H^G

Property 2 makes T^G continue underneath the normal-threshold singularities in channels $g \in G$. However, we also want T^G to continue above the normal-threshold singularities in channels $g \in G = E - G$. Consider, therefore, the functions \bar{T}^G and \bar{T}_H^G defined by the same properties 1, 2, and 3 except that the plus signs in D_g^+ and F^+ are replaced by minus signs. A solution is given by

$$\begin{aligned}\bar{T}^G &= -(T^G)^\dagger \\ \bar{T}_H^G &= -(T_H^G)^\dagger ,\end{aligned}\tag{5.1}$$

and this solution is used.

6. The Good and Bad M^G 's

For certain G 's, called good G 's, the relation $T^G = \bar{T}^G$ holds. In this case M^G is defined by

$$M^G \equiv T^G = \bar{T}^G .\tag{6.1}$$

This function continues underneath the normal threshold singularities for $g \in G$ and continues above the normal threshold singularities for $g \in \bar{G}$.

In general, the relation $T^G - D^G = \bar{T}^G - \bar{D}^G$ holds, and M^G is defined by

$$M^G \equiv T^G - D^G = \bar{T}^G - \bar{D}^G\tag{6.2}$$

where

$$D^G \equiv 0 \quad \text{if } g \in \bar{G} ,\tag{6.3}$$

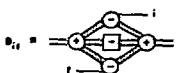
and

$$D^G \equiv \sum_{\{(if)\} \subset X_G} B_{if} \quad \text{if } g \in G ,\tag{6.4}$$

and $D^{-G} = -(\bar{D}^T)^\dagger$. Here

$$X_G \equiv \{(if); \text{ if } g \in G, \text{ if } \bar{G}, \text{ f } \bar{G}\}\tag{6.5}$$

and



$$(6.6)$$

Among the $216 = 65,536$ G 's there are 26,018 good G 's. These are those such that there is no $\{if\}$ such that either $\{(if)cG, tcG, ic\bar{G}, fc\bar{G}\}$ or $\{(if)c\bar{G}, tc\bar{G}, icG, fcG\}$. For good G 's $D^G = \bar{D}^{\bar{G}} = 0$, and hence (6.2) reduces to (6.1)

The good M^G 's are those with good G 's. The bad M^G 's are the rest. The good M^G 's have nice analyticity properties, the bad M^G 's do not. However, the bad M^G 's will be useful nevertheless.

7. Formula for Multiple Discontinuities

Th. multiple discontinuity across the set of cuts H evaluated underneath the set of cuts G (satisfying $G \cap H = \emptyset$) is, by definition,

$$M_H^G \equiv \sum_{H' \subset H} (-1)^{n(H')} M_{H'}^{GH'} \quad . \quad (7.1)$$

This set of formulas is equivalent to the set of formulas (for $G \cap H = \emptyset$)

$$M_H^G = \sum_{G' \subset G} (-1)^{n(G')} M_{HG'} \quad . \quad (7.2)$$

This second form is convenient because most of the M_H^G are zero. Indeed all M_H^G with $n(H) > 3$ vanish, and many of the rest do also. The nonzero M_H^G are now listed.

The function $M_g \equiv M^{\emptyset} \equiv M$ is the connected part of the physical scattering amplitude:

$$M_g = \frac{1}{3} \equiv + \equiv \frac{4}{6} \quad . \quad (7.3)$$

The sixteen single discontinuities M_g are

$$M_i \equiv \begin{array}{c} \text{---} \\ | \\ \text{---} \end{array} \begin{array}{c} \text{---} \\ | \\ \text{---} \end{array} \begin{array}{c} \text{---} \\ | \\ \text{---} \end{array} \quad = \quad \begin{array}{c} \text{---} \\ | \\ \text{---} \end{array} \begin{array}{c} \text{---} \\ | \\ \text{---} \end{array} \quad (7.4a)$$

$$M_r \equiv \begin{array}{c} \text{---} \\ | \\ \text{---} \end{array} \begin{array}{c} \text{---} \\ | \\ \text{---} \end{array} \begin{array}{c} \text{---} \\ | \\ \text{---} \end{array} \quad = \quad \begin{array}{c} \text{---} \\ | \\ \text{---} \end{array} \begin{array}{c} \text{---} \\ | \\ \text{---} \end{array} \quad (7.4b)$$

$$M_{(f)} = \text{Diagram} \quad (7.4c)$$

and

$$M_i = \text{Diagram} \quad (7.4d)$$

It is convenient to introduce special symbols to represent the sum of terms of S (or of S^\dagger) that have special connectedness properties. The symbol defined by

$$\text{Diagram} = \text{Diagram} - \text{Diagram} \quad (7.5)$$

can be shown to represent the sum of the terms of S (or S^\dagger) in which the initial line i is connected to some nontrivial bubble; i.e., it represents the sum of terms in which the line i does not go straight through. Similarly, the symbol

$$\text{Diagram}' = \text{Diagram}' - \text{Diagram}' \quad (7.6)$$

represents the sum of terms of S (or S^\dagger) in which the final line f does not go straight through. Finally, the symbol

$$\begin{aligned} \text{Diagram}' &= \text{Diagram}' \\ &- \text{Diagram}' \\ &= \text{Diagram}' - \text{Diagram}' \quad (7.7) \end{aligned}$$

represents the sum of terms of S (or S^\dagger) in which neither i nor f go straight through. Two frequently used identities, which follow from (7.8), (7.9), and unitarity, are

$$\overline{\square} \square \square \square \square' = - \overline{\square} \square \square' \quad (7.8)$$

and

$$\overline{\square} \square \square \square \square \square' = - \overline{\square} \square \square' \quad (7.9)$$

In terms of these symbols the nonvanishing M_{gh} are given by

$$M_{if} = \overline{\square} \square \square \square \square' \quad (7.10a)$$

$$= - \overline{\square} \square \square \square' \quad (7.10a)$$

$$M_{if} = \overline{\square} \square \square \square \square' \quad (7.10b)$$

$$= - \overline{\square} \square \square \square' \quad (7.10b)$$

$$M_{if} = \overline{\square} \square \square \square \square' \quad (7.10c)$$

$$= - \overline{\square} \square \square \square' \quad (7.10c)$$

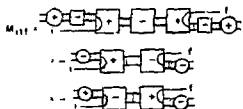
$$M_{ghf} = \overline{\square} \square \square \square \square' \quad (7.10d)$$

$$= - \overline{\square} \square \square \square' \quad (7.10d)$$

$$M_{ghf} = \overline{\square} \square \square \square \square' \quad (7.10e)$$

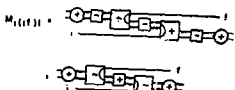
$$= - \overline{\square} \square \square \square' \quad (7.10e)$$

The nonvanishing functions M_{ghk} are



(7.11a)

and



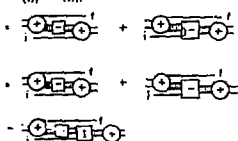
(7.11b)

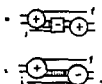
The first form given for each of these functions M_H , although longer than the succeeding ones, exhibits a systematic rule: There is a minus box for each h in H , and these minus boxes occur between the parts of plus boxes that contain nontrivial bubbles on which the appropriate external lines terminate.

8. The Inclusive Optical Theorem

To show how these formulas work we calculate $M_{(if)}^f$, which is the discontinuity across the cut (if) evaluated below the cut f , but above all the other cuts. Using in order equations (7.2), (7.6), (7.8), (7.18), and (7.8), one obtains

$$M_{(if)}^f = M_{if} - M_{ifif}$$





(8.1a)

In a similar way one obtains



(8.1b)

These formulas (8.1) yield the inclusive optical theorem for the three-to-three case.

9. Results for Two-to-Four and Four-to-Two Processes

The results for two-to-four and four-to-two processes are very similar to those for three-to-three processes. Only the definitions of the channels and the formulas for the M_H differ. The nonzero M_H are as follows:

$$M_\phi = \text{---} + \text{---} \quad (9.1)$$

$$M_f = \text{---} + \text{---} = \text{---} + \text{---} \quad (9.2a)$$

$$M_{(ff')} = \text{---} + \text{---} = \text{---} + \text{---} \quad (9.2b)$$

$$M_{\bar{f}} = \text{---} - \text{---} \quad (9.2c)$$

$$M_f(H') = \text{Diagram} = f', \quad (9.3a)$$

$$M_{ff} = + + - - \quad = - - + + \quad (9.3b)$$

$$M_{ffff'} = \text{Diagram} = \text{Diagram} = (9.3a)$$

$$M(f_1'')f_2''' = + \begin{array}{c} \text{---} \\ \text{---} \\ \text{---} \\ \text{---} \end{array} \begin{array}{c} f_1' \\ f_2''' \\ f_1' \\ f_2''' \end{array} = + \begin{array}{c} \text{---} \\ \text{---} \\ \text{---} \\ \text{---} \end{array} \begin{array}{c} f_1' \\ f_2''' \\ f_1' \\ f_2''' \end{array} \quad (9.3d)$$

$$M(FP') \{ F^M \}^{M_1} = \text{Diagram} \quad (9.3e)$$

$$\begin{aligned}
 M_{ff'ff''} &= \text{Diagram with four external lines } f, f', f'', f'''. \\
 &= \text{Diagram with four external lines } f, f', f'', f''' \quad (9.4)
 \end{aligned}$$

The good G 's for the two-to-four case are those such that there is no pair (ff') such that either $\{(ff')eG, teG, f''e\bar{G}, f'''e\bar{G}\}$ or $\{(ff')e\bar{G}, te\bar{G}, f''e\bar{G}, f'''eG\}$. For the good G

$$M^G = T^G = \bar{T}^G \quad (9.5)$$

For all G

$$M^G = T^G - D^G = \bar{T}^G - \bar{D}^G \quad (9.6)$$

where

$$D^G = 0 \quad \text{if } teG \quad (9.7)$$

$$D^G = \sum_{(ff') \in X_G} B_{ff'}, \quad \text{if } teG.$$

Here

$$X_G \equiv \{(ff'): (ff')eG, f''e\bar{G}, f'''e\bar{G}\} \quad (9.8)$$

and

$$B_{ff'} = \text{Diagram with four external lines } f, f', f'', f''' \quad (9.9)$$

The results for the four-to-two case are mirror images of the two-to-four results with i 's in place of f 's.

10. Generalized Steinmann Relations

A pair of channels g and h is said to be overlapping if each of the sets that define g intersect both of the sets that define h . Note that

$$M_H = 0 \quad (10.1)$$

HENRY P. STAPP

if H contains any pair of overlapping channels. Then (7.2) implies that the same is true for M_H^G . These results are a generalization of the Steinmann relations found in field theory: these latter relations give analogous results for the discontinuities formed from 2282 of our 65,536 functions M^G .

VIII. ANALYTIC PROPERTIES OF THE GOOD M^G 's

The good M^G 's defined in the preceding section have nice physical-region analyticity properties. In particular, they continue into themselves around every singularity surface except for certain exceptional ones. This property is the result of systematic cancellations. For each M^G is constructed, according to properties 1 and 2, as a sum of terms only one of which, namely M itself, enjoys this property. All of the remaining terms are represented by bubble diagrams with several bubbles, summed over all possible intermediate lines connecting these bubbles. Each of these remaining terms changes its analytic form at each threshold where a new term, formerly zero, starts to contribute. However, in the sum there is a cancellation of either the plus or minus ϵ part of every threshold singularity, and the function M^G in some neighborhood of the singularity is a limit of an analytic function from some cone of directions in $q = \ln(p + iq)$ space. This result holds, in fact, near all singularity surfaces except the exceptional ones.

Continuation through the physical region is blocked by the exceptional surfaces. However, the functions on the two sides of these exceptional surfaces should be regarded as parts of a single analytic function, in the context of dispersion relations. This will be discussed in the next section. In the present section the continuation of the good M^G around the nonexceptional surfaces is discussed.

1. Schnitts α_g

A schnitt α_g is a schnitt that separates a diagram D into two parts each of which is connected and contains one of the two sets of external lines that define channel g . All lines cut by a schnitt α_g are required to cross the cut in the direction of the positive energy flow in channel g . A schnitt α_g^+ is schnitt α_g each line of which is either a plus line of D or a line of D with no sign. A schnitt α_g^- is defined analogously, with either minus lines or unsigned lines of D . A diagram D contains a schnitt α_g^+ (resp. α_g^-) if and only if it contains a normal threshold diagram D_g^+ (resp. D_g^-).

2. Signs of Lines $V_r \rightarrow V_s$

A line $V_r \rightarrow V_s$ in D is a portion of a flow line in D that runs from V_r to V_s . A sign n is ascribed to $V_r \rightarrow V_s$ if and only if no schnitt α_g^- in D cuts $V_r \rightarrow V_s$.

3. Theorem 14

Consider any B , any D that fits into B , and any line $v_r \rightarrow v_s$ in D that has sign n . In any representation of D

$$w_s - w_r \in V^n, \quad (3.1)$$

where V^+ and V^- are the open forward and backward light-cones, and w_r and w_s are vectors to the space-time location of v_r and v_s , respectively.

Proof Suppose n is plus. If v_r and v_s both lie inside a plus bubble, then each segment on the path between them has a plus sign, hence points into the forward light-cone, and (3.1) follows. If v_r and v_s do not lie inside the same plus bubble then shrink all plus bubble to points. Then almost any vertical line that passes between v_r and v_s defines a schnitt α_g that cuts $v_r \rightarrow v_s$, contrary to hypothesis. An analogous argument holds if n is minus.

4. Skeleton Diagrams

Each Landau diagram D contains a set $G(D)$ of schnitts α_g . A skeleton diagram D_s of D is a minimal subset of the flow lines of D such that $G(D) = G(D_s)$. For three-to-three diagrams there are 76 types of skeleton diagrams:

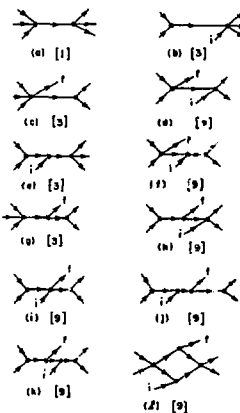


FIG. The 76 skeleton diagrams for 3-3 processes. The indices i and f run over 0, 2, 3, and 4, 5, 6, respectively. The number in square brackets below each figure is the number of skeleton diagrams represented by that figure.

5. Theorem 15

Let $V_r + V_s$ be a line of a skeleton diagram D_s . Let $G(V_r + V_s)$ be the set of g such that some schnitt α_g cuts $V_r + V_s$. Then for every G that contains $G(V_r + V_s)$, for every D with skeleton D_s that fits into a B in \mathcal{B}^G , and for every representation of such a D

$$w_s - w_r \in V^- . \quad (5.1)$$

Proof Consider any D with skeleton D_s that fits into a B in \mathcal{B}^G ; where G contains $G(V_r + V_s)$. This D contains no D_g^+ with g in G , and hence no schnitt α_g^+ with g in $G(V_r + V_s)$. Thus $V_r + V_s$ has a minus sign n , and (5.1) follows from (3.1).

Theorem 15' Theorem 15 holds if \mathcal{B}^G is replaced by $\bar{\mathcal{B}}^G$ and V^- is replaced by V^+ , where $\bar{\mathcal{B}}^G$ is the set of $\bar{B} = -B^+$ for B in \mathcal{B}^G .

6. Continuation of Good M^G 's Around Nonexceptional $L(D)$

Consider any good G . Then

$$M^G = T^G = \sum_{B \in \mathcal{B}^G} B \quad (6.1)$$

and

$$M^G = \bar{T}^{\bar{G}} = \sum_{B \in \bar{\mathcal{B}}^{\bar{G}}} B . \quad (6.2)$$

In considering the singularities of M^G all Landau surfaces $L(D)$ corresponding to diagrams D , having the same type of skeleton D_s will be treated together.

Suppose D_s is a tree diagram. Let $V_r + V_s$ be any minimal line of D_s . Then $G(V_r + V_s)$ will consist of a single element g , which will belong either to G or to \bar{G} .

Suppose $G(V_r + V_s) \subset G$. In this case consider the expression (6.1) for M^G . The structure theorem says that this expression for M^G is singular only on those $L(D)$ corresponding to D that fit into a B in \mathcal{B}^G . If \bar{p} lies only on a subset of these $L(D)$ that all correspond to D 's having skeleton D_s , then Theorem 15 says that for all representations of these D (5.1) holds.

Equation (5.1) precludes the possibility that two $D(p)$'s related to each other by a negative scale change both contribute at $p = \bar{p}$. It is the clash of the prescriptions corresponding to two representations connected by a negative scale change that signals the presence of a threshold, and that is the normal cause for the structure theorem to yield no cone of analyticity near \bar{p} .

The other cases are similar. If D_s is a tree graph and $G(V_r + V_s) \subset \bar{G}$ then use of (6.2) and Theorem 15' leads to essentially the same result as

above, with v^+ replacing v^- . If D_s is a box diagram then for any good G at least two of the four minimal lines $v_r + v_s$ satisfy either $G(v_r + v_s) \subset G$ or $G(v_r + v_s) \subset \bar{G}$, and (3.1) holds for them. Thus negative scale changes are again ruled out.

The above argument rules out, for good H^G , threshold-type singularities generated by a pair of $D(\bar{p})$ related by a negative scale change. However, the continuation might be blocked by some other conspiracy of singularities. One can show, however, by dimensional considerations, that the only conspiracies that can block the continuation near \bar{p} are those involving two diagrams $D_1(p)$ and $D_2(p)$ whose external trajectories are transformed into each other by a negative scale change for each p in some codimension-one neighborhood of \bar{p} . On the other hand, the D_1 and D_2 must conform to the sign conditions (3.1) derived above. Surfaces generated $D_1(p)$ and $D_2(p)$ satisfying these conditions are called exceptional. The occurrence of such exceptional surfaces appears to be essentially accidental and of no great significance for dispersion relations. This will be discussed in the next section.

IX. ANALYTICITY IN THE COMPLEX MASS SHELL

The physical-region analyticity properties discussed above flow from unitarity and macrocausality. To obtain analyticity properties at nonreal points an additional assumption is needed. In S-matrix theory this extra assumption is maximal analyticity, which says that the only singularities of the scattering amplitude are those required for consistency with the other S-matrix principles of unitarity, macrocausality, and Lorentz invariance. This assumption, and several of its consequences, are discussed in this section.

1. Maximal Analyticity

Unitarity and macrocausality yield the physical-region analyticity properties described in the preceding sections. Maximal analyticity says that there are no singularities in the complex mass shell not required for consistency with these physical-region analyticity properties and Lorentz invariance. This assumption has two levels. On the deeper "bootstrap" level it refers to a complete solution to the unitarity, analyticity, and Lorentz invariant requirements that may in principle determine all the parameters of the S-matrix, i.e., the masses, and coupling constants etc. But on the immediate practical level it refers to the analyticity properties associated with given values of the masses. On this latter level it means, in practice, an iterative procedure whereby the singularity structure in the complex mass shell is built up starting from the basic normal threshold cuts. In this procedure one first neglects all cuts but the normal threshold cuts, and then derives further cuts and singularities by introducing these normal threshold cuts into the unitarity equations. These new singularities are then themselves introduced into unitarity

and further singularities are derived, etc. At each stage one considers only those singularities that have arisen in the previous stages, and expects to generate in the end the complete analytic structure.

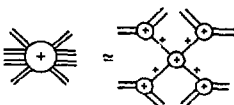
This iterative procedure has two parts. In the first part one considers only stable particles (in an approximation where massless particles, and hence electromagnetic, weak, and gravitational interactions are ignored) and seeks to generate only the physical-sheet analytic structure. This is the sheet in which dispersion relations operate, and hence the sheet of principal interest here. In the second part one allows unstable particle poles, and seeks to generate the analytic structure on all sheets.

The initial stages of this iterative procedure are described in the following subsections, and are used to obtain hermitian analyticity, crossing, and certain other properties needed for dispersion relations.

At the first stage of the iterative procedure one considers only the normal threshold singularities and cuts, which include the pole singularities associated with one-particle exchange diagrams. The pole-factorization theorem is used extensively, and it is assumed that no singularities associated with other types of diagrams mask or simulate these one-particle exchange pole singularities. That is, it is assumed that the only singularities of bubble diagram functions that contribute to residues of poles at the particle masses $p_a^2 = m_a^2$ are singularities associated with the corresponding one-particle exchange diagrams. If at some stage of the construction of the singularity structure a singularity is found that disrupts this property then it should be taken into account at the subsequent stages, but not before. However, no such singularity has ever been found.

2. Hermitian Analyticity

This property says that the functions represented by the plus and minus bubbles are analytic continuations of each other. To show this for a two-to-two process consider a larger process whose amplitude contains the two-to-two amplitude as a factor of a four-fold multiple-pole residue. The scattering amplitude for the larger process is represented by the bubble on the left-hand side of



The original two-to-two processes is represented by the central bubble on the right-hand side.

Consider now the unitarity equation

$$\begin{array}{c}
 \text{Diagram: Two vertical lines with internal labels } +, -, +, - \text{ and } - \text{ and } +, - \text{ and } +, - \text{ on the left. A central vertical line labeled } I \text{ is connected to the right. The right side is a vertical line labeled } c. \\
 - \\
 \text{Diagram: Two vertical lines with internal labels } +, -, +, - \text{ and } - \text{ and } +, - \text{ and } +, - \text{ on the left. A central vertical line labeled } I \text{ is connected to the right. The right side is a vertical line labeled } c. \\
 = 0
 \end{array}
 \quad (2.2)$$

where the subscript c denotes connected part. It can be separated to four terms

$$\begin{array}{c}
 \text{Diagram: Two vertical lines with internal labels } +, -, +, - \text{ and } - \text{ and } +, - \text{ and } +, - \text{ on the left. A central vertical line labeled } I \text{ is connected to the right. The right side is a vertical line labeled } c. \\
 + \\
 \text{Diagram: Two vertical lines with internal labels } +, -, +, - \text{ and } - \text{ and } +, - \text{ and } +, - \text{ on the left. A central vertical line labeled } I \text{ is connected to the right. The right side is a vertical line labeled } c. \\
 - \\
 \text{Diagram: Two vertical lines with internal labels } +, -, +, - \text{ and } - \text{ and } +, - \text{ and } +, - \text{ on the left. A central vertical line labeled } I \text{ is connected to the right. The right side is a vertical line labeled } c. \\
 + \\
 \text{Diagram: Two vertical lines with internal labels } +, -, +, - \text{ and } - \text{ and } +, - \text{ and } +, - \text{ on the left. A central vertical line labeled } I \text{ is connected to the right. The right side is a vertical line labeled } c. \\
 + R = 0
 \end{array}$$

where R is the sum of contributions to (2.2) not appearing in any of the first three terms. For brevity this equation is written

$$A_+ - A_- - A_0 + R = 0. \quad (2.3)$$

The term R gives no contribution to the four-fold multiple-pole at $p_\alpha^2 = m_1^2$. The contributions of the first three terms are displayed in the equations

$$A_+ = \begin{array}{c} \text{Diagram: Two vertical lines with internal labels } +, -, +, - \text{ and } - \text{ and } +, - \text{ and } +, - \text{ on the left. A central vertical line labeled } I \text{ is connected to the right. The right side is a vertical line labeled } c. \\ + \\ \text{Diagram: Two vertical lines with internal labels } +, -, +, - \text{ and } - \text{ and } +, - \text{ and } +, - \text{ on the left. A central vertical line labeled } I \text{ is connected to the right. The right side is a vertical line labeled } c. \\ - \\ \text{Diagram: Two vertical lines with internal labels } +, -, +, - \text{ and } - \text{ and } +, - \text{ and } +, - \text{ on the left. A central vertical line labeled } I \text{ is connected to the right. The right side is a vertical line labeled } c. \\ + R_+ \end{array}$$

Equation (2.4) continued

$$\begin{aligned}
 A_- &= \text{Diagram with a minus sign on line } L_1 \text{ (top line)} + R_- \\
 A_0 &= \text{Diagram with a plus sign on line } L_1 \text{ (top line)} + R_0
 \end{aligned}
 \tag{2.4}$$

A plus or minus sign σ_i on a line L_i of a bubble diagram signifies the restriction of essential support of the displayed function to the part generated by the indau equations with the restriction $\sigma_i \sigma_i > 0$. This means that the mass- ϵ Δ delta function associated with this line is replaced by a pole, according to the rules

$$\begin{aligned}
 + &\approx i/p_a^2 - m_a^2 + i\epsilon \\
 - &\approx -i/p_a^2 - m_a^2 - i\epsilon
 \end{aligned}
 \tag{2.5}$$

in the sense that the displayed function in a neighborhood of one of these singularities is represented by a function having a pole factor of the indicated type (2.5) and having the indicated residue. This residue is the product of the displayed bubble function, times a factor of plus i for each plus line and a factor of minus i for each minus line. These factors of i come from the residues of the pole factors (2.5).

The remaining terms R_+ , R_- , and R_0 in (2.4) have no four-fold multiple-pole contribution at $p_a^2 = m_a^2$, $a = 1, \dots, 4$.

The momentum-energy variable p_a is the momentum-energy variable associated with internal line a :

$$p_a \equiv \sum_{i \in E_a} \epsilon_i p_i
 \tag{2.6}$$

where E_a is the set of labels i of the external lines of the outer bubble connected to line a .

Multiplication of (2.3) by the factor

$$\prod = \prod_{a=1}^4 (p_a^2 - m_a^2)
 \tag{2.7}$$

gives

$$A'_+ - A'_- - A'_0 + R' = 0 \quad (2.8)$$

$$\text{where } A'_+ = \prod A'_+ \text{ etc.}$$

Each of the three central functions in (2.4) has certain singularities in the complex mass-shell of the four particles $\alpha = 1, \dots, 4$. When variable $p = (p_1, \dots, p_{16})$ goes to the pole position $p_\alpha^2 = m_\alpha^2$, $\alpha = 1, 2, 3, 4$, the singularities of these central functions in (2.4) will produce singularities in the corresponding primed functions in (2.8). These latter singularities cannot be present at $p_\alpha^2 = m_\alpha^2$ but absent at nearby points $p_\alpha^2 \neq m_\alpha^2$: there is a general theorem of functions of several complex variables (Bremermann's special continuity theorem) that rules this out.

These neighboring singularities of the primed functions are associated with the Landau diagrams of the larger process in which the four intermediate pole lines in (2.4) are contracted to points. These contributions to the singularities of the primed functions are represented by the first terms in the equations

$$A'_+ = \text{Diagram} + R'_+ \quad (2.9)$$

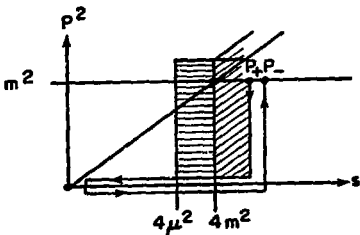
$$A'_- = \text{Diagram} + R'_- \quad (2.10)$$

$$A'_0 = \text{Diagram} + R'_0 \quad (2.11)$$

Each first term represents a function that becomes equal to the displayed product of bubble functions at the mass-shell points $p_\alpha^2 = m_\alpha^2$, $\alpha = 1, \dots, 4$, and that outside these mass-shell points has only singularities corresponding to the Landau diagrams that fit into these bubble diagrams. The remaining terms R'_+ , R'_- , and R'_0 have no singularities corresponding to diagrams that fit into these bubble diagrams, and they vanish at the mass shell points $p_\alpha^2 = m_\alpha^2$.

$\alpha = 1, \dots, 4$, along with their discontinuities. The equations (2.9), (2.10), and (2.11) represent essentially decompositions of the singularities of A'_+ , A'_- , and A'_0 into those that have discontinuities having nonzero multiple-residue at $p_\alpha^2 - m_\alpha^2 = 0$, $\alpha = 1, \dots, 4$, are those that do not.

Consider now a path in the variables of the larger process



The variable s is the square of the center-of-mass energy of the central process. The variable p^2 is the common value of the variables p_α^2 , and m^2 is the (assumed common) value of the m_α^2 . The t variable of the central process can be fixed at zero, and the other variables of the larger process changed in some minimal way that keeps all momentum-energy vectors p_i real, except near infinitesimal if distortions around singularity surfaces.

Let P_+ be a mass-shell ($p_\alpha^2 = m_\alpha^2$, $\alpha = 1, \dots, 4$) point lying above the physical threshold at $s = 4m^2$. Let A'_+ be continued first at constant s from $p^2 = m^2$ to $p^2 = 0$, and then at constant $p^2 = 0$ to $p^2 = s = 0$. This path will follow a plus ic (physical) continuation around the singularities associated with the plus bubbles of (2.9) and a minus ic (antiphysical) continuation around the singularities associated with the minus bubbles of (2.9). The path is allowed, however, to pass through cuts corresponding to singularities of the function R'_+ of (2.9). In crossing such a cut the function A'_+ changes by just the discontinuity of R'_+ across this cut. In this way the function on the path remains always the function A'_+ defined above.

At the point $p^2 = s = 0$ the term A'_0 vanishes, because this point lies below the lowest threshold $s = 4\mu^2$ in the s channel. Thus by adding R' , which can be considered to be the discontinuity across a cut, one obtains the function A'_- , which is then continued at $p^2 = 0$ back to $s > 4m^2$, and then at constant s to the mass shell point P_- . Thus one has a path that follows

well-defined ic rules for singularities corresponding to diagrams having the four vertices a , but that jumps across cuts associated with the functions R'_+ , R' , and R'_- .

Let this path of continuation now be shifted into the mass shell $p^2 = m^2$. In this shift of the path of continuation one keeps track of the various cuts of the functions R'_+ , R' , and R'_- , that the path jumps across, but does not seek to avoid them: instead one adds the discontinuities across these cuts. However, one does try to distort the path away from singularities corresponding to diagrams that have the four vertices a .

In tracing out the distortion of the path one may consider the five parts separately; one traces out the motion of the singularity surfaces of the individual bubbles of (2.9), (2.10), and (2.11) as the "mass variable" p_a^2 corresponding to the vertices a increase from zero to m_a^2 .

Consider first the path in the variables of the central bubble. For $p^2 = 0$ this path starts at a point $s = 4m^2 + c$ above threshold, continues down to $s = 0$, crosses the line $\text{Im } s = 0$, and continues back. As one shifts p^2 from zero to m^2 certain singularities may cut across this original path in the s plane and force a distortion. However, in the first stage of the iterative procedure one considers only normal threshold singularities. These stay fixed in the s plane and hence cause no distortion of the path. Normal thresholds in p^2 must lie at $p^2 > m^2$, and hence are not encountered in the continuation.

Consider next the paths in the variables of the outer bubbles. These can be made to trace exactly the same paths along the original and return portions of the part between $p^2 = m^2$ and $p^2 = 0$ at fixed $s > 4m^2$. Moreover, since the invariant variables of the outer parts are independent of s one can keep the same path in the space of invariants for all s .

After the path is shifted into the mass shell, which is certainly possible at the first stage of the iteration procedure, one has a mass-shell path of continuation that connects the residue at P_+ to the residue at P_- . This path jumps across various cuts of the functions R'_+ , R' , and R'_- , but the discontinuities across these cuts vanish on the mass shell $p_a^2 = m_a^2$ $a = 1, \dots, 4$. Thus the analytic continuation of the residue at P_+ along the mass-shell path to the point P_- yields the residue at P_- .

The residue at P_+ is, by virtue of the pole-factorization theorem, the product of the five functions represented by the first term of (2.9). Similarly the residue at P_- is the product of the five functions represented by the first term of (2.10).

The five functions in the residue at P_+ continue independently. The variables of the outer processes remain always at the same point in the space of the invariants, and trace out only a trivial path in p space. Thus in the continuation from P_+ to P_- the outer functions continue into themselves, and hence into the outer functions occurring in the residue at P_- . Therefore the inner function must continue from its value in the residue at P_+ to its value in the residue at P_- . That is, the function represented by the plus bubble must continue into the function represented by the minus bubble. The path of continuation in the variables of the central process, is, at the first stage of the construction of the singularity structure in the complex mass shell, a path that starts at a physical point above the physical threshold $s = 4m^2$, moves in the upper half plane (i.e. via the plus ic rule) to $s = 0$, where it moves into the lower half plane and returns via the minus ic rule to the region $s > 4m^2$. This relation between the plus and minus bubbles is called hermitian analyticity.

At a later stage of the construction of the singularity structure some singularity may move across the original s -plane path of continuation during the shift from $p^2 = 0$ to $p^2 = m^2$, and cause a distortion of the path away from its original position. An example will be given later. But at the initial stage, where only normal threshold cuts are considered, the plus and minus bubbles represent two different boundary values of the same analytic function.

The same argument works for multiparticle amplitudes, and shows that our good functions M^G are the boundary values indicated by G of a single analytic function, at least at the first stage of the construction of the complex singularity structure. To obtain this result the larger space is constructed by replacing each line of the 6-particle process by four lines, as in (2.1). The needed equation in this larger space can be constructed, in the formal framework, by defining the functions T_H by the same equations in terms of B_i^+ as before, but with the T 's now functions in this larger space, and the D_g^+ 's now the natural images of the original D_g^+ 's in this larger space. The argument then proceeds as just before.

As an example consider the case where $g = i - \epsilon$ designates an initial subenergy channel. It is sufficient to enlarge the process only with respect to the two initial lines 2 and 3. As before, the T of the enlarged process is continued first from P_+ to $p_2^2 = p_3^2 = 0$, at fixed $s_{23} = (p_2 + p_3)^2$ and then to $s_{23} = p_2^2 = p_3^2 = 0$. At this point the discontinuity function $T_g = T_1$ vanishes, and T can be replaced by $T - T_g = T^g$, modulo R-type functions, which are functions that lack the double pole at $p_2^2 = m_2^2$, $p_3^2 = m_3^2$. Then $T^g = T - T_g$ is continued back to P_- , following the ic prescription appropriate to it, and jumping across R cuts, and also across the cuts attached to exceptional surfaces, by adding the appropriate discontinuities. Finally the

path is distorted into the mass shell $p_2^2 = m_2^2$, $p_3^2 = m_3^2$, and the residues the double pole in T and $T - T_g$ considered. These two functions are analytically connected by the mass-shell path obtained by distorting into the mass shell the original $p_1^2 = p_2^2 = 0$ path in the s_{23} plane. That original path starts in $s_{23} > (m_2 + m_3)^2$, then runs down to $s_{23} = 0$ following the plus ic rule for singularities not of R type, and then runs back to $s_{23} < (m_2 + m_3)^2$ following the ic rules appropriate to $T^8 = M^8$. Again the two outer factors can be factored out, leaving the analytic connection between T and $T - T_g$ in the space of the six original particles. This path jumps across cuts attached to exceptional surfaces. The placement of such cuts will be discussed later.

By similar arguments one can derive

$$\alpha \text{---} \text{circle with } \alpha \text{---} \gamma = \left(\text{---} \text{box } a \text{---} \text{box } -a \text{---} \text{box } \beta \text{---} \text{circle with } c \text{---} \gamma \right) \quad (2.12)$$

where the left-hand side represents the continuation of $S_c(\alpha, \beta; \gamma)$ to below the complete set of cuts that start at the threshold point

$$s_a^0 = \left(\sum_{i \in a} m_i \right)^2. \quad (2.13)$$

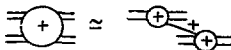
The $-a$ box is, as before, an operator in a space, which is the space of sets of particles the sum of whose masses is s_a^0 , and is the inverse of the restriction of the S-matrix to this space. In deriving (2.12) the original path in the variables of the larger process can be taken to lie at $p_a^2 = m_a^2 - \epsilon$, with ϵ arbitrarily small, instead of at $p_a^2 = 0$, and to describe an infinitesimal contour in the space of variables of the central process, since this small contour is enough to take it into the region $s_a < s_a^0$, where the threshold term vanishes. Thus the continuation that connects $S_c(\alpha, \beta; \gamma)$ to the function represented on the left-hand side of (2.12) is nondistorted; it is an infinitesimal circle around the threshold point that is the continuation into the mass-shell of a infinitesimal circle originally defined for $p_a^2 = m_a^2 - \epsilon$, for $\epsilon > 0$.

3. Crossing

Crossing is the property whereby the analytic continuation of the scattering function for any given process describes also the various processes related to it by changing various sets initial particles into final antiparticles, and vice versa. It is derived by methods very similar to those just described, so a

very brief description will suffice.

Consider, for example, a pole in a four-to-four amplitude

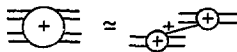


(3.1)

This pole lies at $p_\alpha^2 = m_\alpha^2$, where

$$p_\alpha = \sum_{i \in E_\alpha} e_i p_i$$

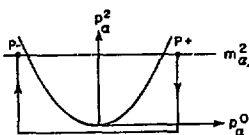
is the exchanged momentum-energy. If the exchanged particle has an antiparticle then this same four-to-four amplitude will have, in another portion of its physical region, another pole at $p_\alpha^2 = m_\alpha^2$:



(3.2)

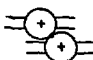
The first pole lies in the region $p_\alpha^0 > m_\alpha$ whereas the second lies in $p_\alpha^0 < m_\alpha$. The intervening region along $p_\alpha^2 = m_\alpha^2$ lies outside the physical region.

Let f^+ be the four-to-four scattering amplitude, and consider the continuation of the residue function $(p_\alpha^2 - m_\alpha^2)f^+$ along the path indicated below:



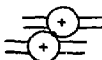
(3.3)

This continuation starts a mass-shell point P_+ , at which the residue function is i times



(3.4)

and moves, staying always in the physical region of f^+ , to a mass-shell point P_- , at which the residue function is i times



(3.5)

Let this path now be shifted into the mass shell $p_\alpha^2 = m_\alpha^2$, jumping across all cuts of the R-type, which are cuts corresponding to diagrams that are not separated into parts in the manner indicated in (3.4) and (3.5). As before, the discontinuities of the residue function across these R-type cuts will vanish at $p_\alpha^2 = m_\alpha^2$, because they do not correspond to one-particle exchange diagrams, and hence lack the pole singularity. However, the discontinuity across the singularities corresponding to diagrams that fit into the bubbles (3.4) and (3.5) will be nonzero, in general, and should be avoided, if possible.

At the first stage of the procedure for building up the singularity structure the path of continuation can certainly be shifted into the mass shell, for the only normal threshold singularity that could block the shift would be one in the variable p_α^2 , whereas the point $p_\alpha^2 = m_\alpha^2$ lies below the lowest communicating normal threshold in this channel, by virtue of the stability of particle α .

If the path can be shifted into the mass shell then the product represented by (3.4) continues into the product represented by (3.5). The individual factors are functions of different variables and hence they also continue into each other, modulo constant factors c and c^{-1} .

These factors c and c^{-1} can be taken to be unity. To see this let $c = c_1$ be defined by

$$f(\dots; \dots p_1^c) = c f^+(\dots; \dots \bar{p}_1^c; \dots) \quad (3.6)$$

and

$$f(p_1^c \dots; \dots) = c^{-1} f^+(\dots; -\bar{p}_1^c \dots) \quad (3.7)$$

where the functions on the left-hand sides represent the continuations of

$f^+(\dots; \dots p_i)$ and $f^+(p_i \dots; \dots)$, respectively, from their original physical regions along an on-mass-shell crossing path to the real point p_i^c , which has negative energy component, and the bar over \bar{p}_i^c indicates that the associated suppressed type-variable is $\bar{t}_i = -t_i$, which designates the antiparticle of the particle of type t_i . Continuation of (3.6) along the path of hermitian conjugation of the function on the right gives

$$\begin{aligned} f(\dots; \dots p_i^{ch}) &= cf(\dots; \dots \bar{p}_i^{ch}; \dots) \\ &= cf^-(\dots; \dots \bar{p}_i^{ch}; \dots) \\ &= c(-f^+(\dots; \dots \bar{p}_i^{ch}))^* . \end{aligned} \quad (3.8)$$

On the other hand, the continuation of $f^+(\dots; \dots p_i)$ along its path of hermitian conjugation gives

$$\begin{aligned} f(\dots; \dots p_i^h) &= f^-(\dots; \dots p_i^h) \\ &= -(f^+(\dots; \dots p_i^h))^* . \end{aligned} \quad (3.9)$$

Continuation of (3.9) along the path of crossing of the function on the right-hand side gives, by virtue of (3.7) (and bose statistics),

$$f(\dots; \dots p_i^{hc}) = -(c^{-1} f^+(\dots; \dots \bar{p}_i^{hc}))^* . \quad (3.10)$$

The paths ch and hc are homotopically equivalent, at least at the first stage of the iterative procedure. Hence the points p_i^{ch} and p_i^{hc} represent the same points on the Riemann surface. Thus comparison of (3.8) and (3.10) yields

$$c = (c^{-1})^* ,$$

which says that $c = c_i$ is a phase factor: $c_i = \exp i\phi_i$.

Because of the factorized form of (3.4) and (3.5) this phase factor c_i depends only on the type t_i of the particle exchanged. This factor may be removed completely by redefining the phase of the S-matrix:

$$\begin{aligned} S(p_1, \dots, p_m; p_{m+1}, \dots, p_n) &\rightarrow S'(p_1, \dots, p_m; p_{m+1}, \dots, p_n) \\ &= S(p_1, \dots, p_m; p_{m+1}, \dots, p_n)C \end{aligned}$$

where

$$C = \prod_{i=1}^m \exp \left(-i \frac{1}{2} \sum_i \epsilon_i \phi_i \right)$$

and

$$\epsilon_i = -1 \quad \text{for } i = 1, \dots, m$$

$$c_i = +1 \quad \text{for } i = m+1, \dots, n \quad .$$

The phases will always be chosen so that the c_i are unity.

The above arguments yield hermitian analyticity and crossing only at the first stage of the iterative procedure for building up the singularity structure in the complex mass shell, but this is all that is needed to start the procedure going. At later stages certain cuts generated by the iterative procedure may block the continuations, but these cuts, since they are generated by unitarity should, in principle, have their discontinuities determined by unitarity. If they do then it is not important whether they block or do not block the paths of crossing and hermitian analyticity.

4. Triangle Diagram Cuts

The second stage of the iterative procedure generates cuts associated with triangle diagram singularities

Consider, for example, the six-particle function f as a function of one initial subenergy σ , with seven other variables s_g held fixed and nonreal. At the first stage of the iterative procedure the function f near the σ normal threshold can be represented by the Cauchy formula with a principal contribution

$$\int_{4m^2}^{\infty} \frac{d\sigma'}{2\pi i} \frac{\text{Disc}_\sigma f(\sigma')}{(\sigma' - \sigma)} \quad (4.1)$$

The discontinuity is given by

$$\text{Disc}_\sigma f(\sigma') = \text{Diagram} \quad (4.2)$$

Let Δ represent some triangle diagram

$$\Delta = \text{Diagram} \quad (4.3)$$

and consider the discontinuity of (4.2) around $L(\Delta)$. The discontinuity of a bubble diagram function F^B around a singularity surface $L(D)$ is obtained by summing, over all ways that D fits into B , the discontinuity associated with

this particular way. This latter discontinuity is obtained by replacing each bubble b of B by the discontinuity function associated with the part D_b of D that fits into b .

In our case the diagram Δ fits into (4.2) in two ways. In the first way the initial vertex fits into the minus bubble and the other two vertices fit into the plus bubble. In the second way the leading vertex is considered to be a contraction of several vertices, one of which fits in the minus bubble, and the rest of which fit into the plus bubble. (Only unsigned lines can be contracted.) Actually these latter diagrams D are different from Δ but, because of the contraction of vertices, the surfaces coincide, and they should be considered together.

The sum of contributions corresponding to these various ways of fitting Δ into (4.2) is

$$\begin{aligned}
 & \text{Diagram 1:} \\
 & \text{Diagram 2:} \\
 & \text{Diagram 3:} \\
 & = \text{Disc}_\Delta \text{ Disc}_G f \quad . \quad (4.4)
 \end{aligned}$$

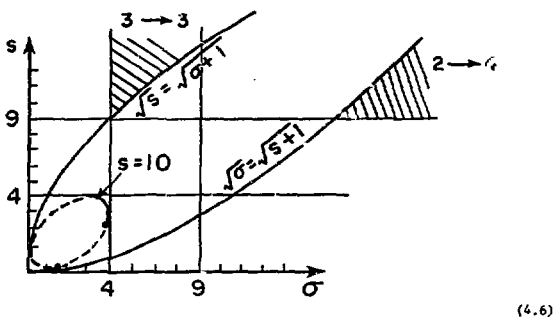
The diagrams are Feynman-like graphs. Diagram 1 shows a horizontal line with a minus sign at the left end, followed by a wavy line labeled α , then a plus sign, and finally a wavy line labeled β . A vertical line labeled γ connects the α and β segments. Diagram 2 shows a similar structure but with a plus sign at the left end and a minus sign at the right end. Diagram 3 shows a triangle with vertices labeled α , β , and γ . The edges are wavy lines. The labels α , β , and γ are placed near the vertices or edges of the diagrams.

Note that

$$\text{Disc}_\Delta \text{Disc}_\sigma f = \text{Disc}_\Delta f \quad (4.5)$$

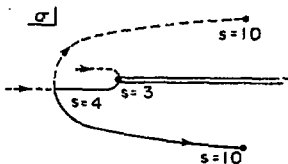
This relation (4.5) means that the surface $L(\Delta)$ need not be singular on all sheets of the σ cut: the Δ singularity can be "shielded" by the σ cut, and not appear on all sheets.

Consider, for simplicity, a theory with all masses equal. Then the physical region in the real $\sigma - s$ plane consists of the two shaded regions in



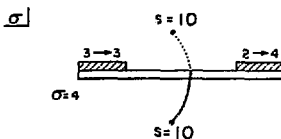
The little oval in the 4-by-4 box represents the location of the triangle diagram singularity for the case in which each set of lines α , β , and γ of Δ consists of one line. A condition on the singularity structure entailed by the arguments of the preceding subsections is that if the singularity structure is formally continued off-mass-shell to a neighborhood of the origin $p = 0$, then that neighborhood should be free of singularities. This condition entails that the dotted portion of the triangle singularity not be present on the physical sheet: it must lie on an unphysical sheet of the σ cut.

Tracing the motion of the Δ singularities in the σ plane as s increases from a value slightly less than three, and moves on a path infinitesimally above the real axis, one finds



(4.7)

where the solid line represents the physical-sheet part of the trajectory. This path is also traced out in (4.6). The two singularities of the discontinuity function (4.4) at each value of σ are connected by a cut, which is here pictured for $s = 10$:



(4.8)

This cut separates the real σ axis into two parts, in which lie the $3 + 3$ and $2 - 4$ physical regions. The discontinuity formula in the $3 + 3$ physical region is represented by



(4.9)

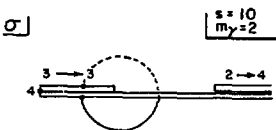
whereas that in the $3 \rightarrow 4$ physical region is represented by



(4.10)

This cut that separates the two physical regions of the discontinuity function does not separate the two physical regions of the scattering function itself: they are connected by a direct path that remains always near the real σ axis. This is because the part of the cut in the discontinuity that lies in the upper-half σ plane lies on the unphysical sheet of the scattering function. On the other hand, the part of this cut that lies in the lower-half σ plane extends into the physical sheet of the scattering functions, and hence gives an extra contribution to the dispersion (i.e., Cauchy) formula.

As one formally increases the mass m_γ of line γ in Δ the tip of the cut curls around and at $m_\gamma = 2$ it touches the underside of the $3 \rightarrow 3$ physical region:



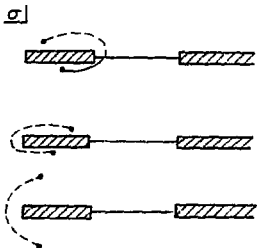
(4.11)

This singularity sits in the region associated with the function M^g , where g identifies the σ cut that we have been discussing. The continuation of M^g is blocked by this singularity surface, which is one of the exceptional surfaces mentioned in earlier sections.

This surface does not cause any serious difficulty for dispersion relations. In the principal contribution to the Cauchy formula, i.e., in the contribution from the normal threshold cut, one uses the normal threshold discontinuity formula (4.8) or (4.10) at all points along the cut. However, there is also the contribution corresponding to the loop in the lower-half plane of (4.11). The discontinuity across this latter cut is given by (4.5).

This relatively simple situation can be contrasted to conceivable ones in which the singularity lies at the end of a cut that bounds the physical sheet and extends to infinity, and for which no discontinuity formula is known. Such a cut would add an uncontrolled contribution to the dispersion relation.

As the mass m increases above 2, with a small negative imaginary part, the Δ diagram cut passes through the sequence of positions shown below ($a = 10$)



That is, it rapidly retreats from the physical sheet, and then moves, in the unphysical sheet, away from the real axis.

The situation indicated in (4.11) occurs when $m_Y = m_\rho + 1$, and σ and s are large enough so that the process represented by the triangle diagram (4.3) is physical. Thus as the masses m_α , m_β , and m_Y increase these singularities move to larger values of s and σ . The physical-sheet parts of the Δ cuts are confined to a neighborhood of the gap between the two physical regions that grows only as $\sqrt{\sigma}$ (or \sqrt{s}). Hence these singularities become increasingly localized on rays that run almost parallel to the line $\sigma = s$: they do not go into the region where $\sigma \gg s$ or $s \gg \sigma$. This is true both for the case above, where $m_Y > m_\rho$ and the cut curls into the $3 \sim 3$ region, and also for the case $m_\rho > m_Y$ where the cut curls into the $2 \sim 4$ region. This localization of these complex cuts will be used in the discussion of the generalized fixed- t dispersion relations.

5. Higher Cuts

All diagram cuts and higher-order cuts are generated by the same procedure. Box

diagram cuts sometimes protrude from triangle diagram cuts, etc. In the examples studied so far nothing happens that is significantly different from what happened in the δ case, and all the new physical-region cuts appear to be localized in the neighborhood of the gap.

REFERENCES TO PROOFS OF THEOREMS

Theorem 1 is Theorem 5 of Chandler (1). Theorem 2 is trivial. Theorem 3 is proved in Stapp (10). Pham's Theorem is proved in Pham (9). Theorem 4 is part of Theorem 6 of Chandler (1). A similar result at nonpositive- α points is proved in Section 3 of Coster (2) (see (3.10) of that reference). A still more general version is lemma A9 of Appendix A of Coster (5). Theorem 5 is Theorem 7 of Chandler (1). Theorem 6 is contained in Theorem 6 of Chandler (1). The connection between Landau surfaces and space-time diagrams is discussed in detail in Chandler (1), in Coster (2), and in Iagolnitzer (8).

The formal method is developed in Coster (4) and in Coster (5), where the uniqueness of the T_G and T^G is shown. The general formula for the discontinuity of f^+ around $L_0(D^+)$ is derived by finite methods in Coster (2) for all points lying below the lowest 4-particle threshold. The results (4.1) and (5.1) of Section V are Eqs. (B3) and (5.7) of Coster (3). The properties of the $-\alpha$ box are described in detail in Coster (3), where α is replaced by i .

The discussion given here is more general than that of the earlier works in that it uses the newer stronger version of the structure theorem recently proved by Iagolnitzer, and discussed in the preceding series of lectures. This allows some unnecessary assumptions to be eliminated.

The proof of hermitian analyticity and crossing is essentially the argument of Olive, which is described in Eden (4), and developed in Stapp (11). The discussion of the triangle diagram cuts is based on the work of Hwa (7).

REFERENCES

- (1) C. Chandler and H. P. Stapp, J. Math. Phys. 10 (1969) 826.
- (2) J. Coster and H. Stapp, J. Math. Phys. 10 (1969) 371.
- (3) J. Coster and H. Stapp, J. Math. Phys. 11 (1970) 1441.
- (4) J. Coster and H. Stapp, J. Math. Phys. 11 (1970) 2743.
- (5) J. Coster and H. Stapp, J. Math. Phys. 16 (1975) 1288.
- (6) R. J. Eden, P. V. Landshoff, D. I. Olive, and J. C. Polkinghorne, *The Analytic S-matrix* (Cambridge University Press, 1966).
- (7) R. Hwa, Phys. Rev. 134B (1964) 1086.
- (8) D. Iagolnitzer, *Introduction to S-matrix Theory* (North-Holland) to be published.

HENRY P. STAPP

- (9) F. Pham, Ann. Inst. Henri Poincaré 6 (1967) 89.
- (10) H. P. Stapp, J. Math. Phys. 8 (1967) 1606
- (11) H. P. Stapp, J. Math. Phys. 9 (1968) 1548.